JPSS/NPP ATMS SDR REVIEW

NASA CalVal Report

C.-H. Joseph Lyu & Ed Kim

NASA/GSFC

Jan. 13, 2012

1. Introduction

The NPP satellite was launched on Oct. 28, 2011. The Advanced Technology Microwave Sounder (ATMS) has been in operational mode since Nov. 8, 2011. In this first post-launch ATMS sensor performance report, NASA Cal/Val team would focus on the review of the assigned Cal/Val Tasks, indicated in "ATMS SDR Validation OPSCON and Cal/Val Task Description" (May 24, 2011) document, listed below.

1) Task 3 – Functional Evaluation, in Sec. 2.
2) Task 4 – **Optimal Space View Determination**, in Sec. 3.
3) Task 8 – Scan Angle, in Sec. 4.
4) Task 9 – Radiometric Sensitivity, in Sec. 5.
5) Task 14 – **Lunar Intrusion Mitigation**, in Sec. 6.

Moreover, we would review also some important, **urgent and SDR related** issues in Secs. 7 & 8. In Sec. 9, Concluding Remarks, we summarize our results, recommendations and suggestions. Before presentation, for entertaining, we would like to show some **amazing ATMS snow/rain/ice global image**.

The **Blizzard Storm** in USA Mid-West & Rains (18 *mm* H_2O) in the NW/E coast. **Ch 17** sees a combination of the **surface** plus **water vapor** and **ice** crystals in the atmosphere.

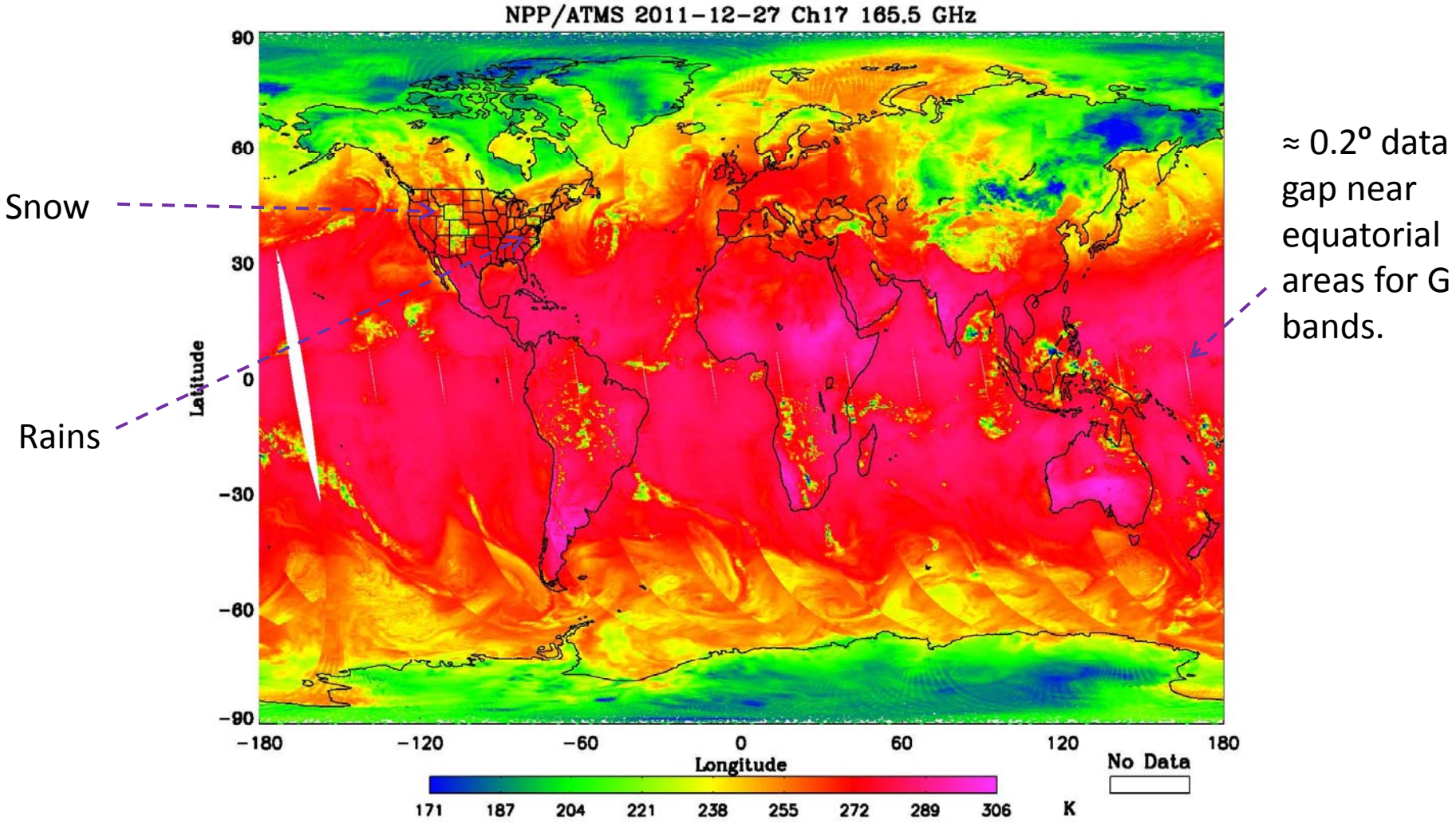

NASA ATMS Global Image

More ground coverage than previous MW sensors.

Corresponding USA/Canada/Mexico **Weather Forecast Map** on 12-27-2011

316
309
303
297
291
284
278
272
266
259
253
253
247
..K..

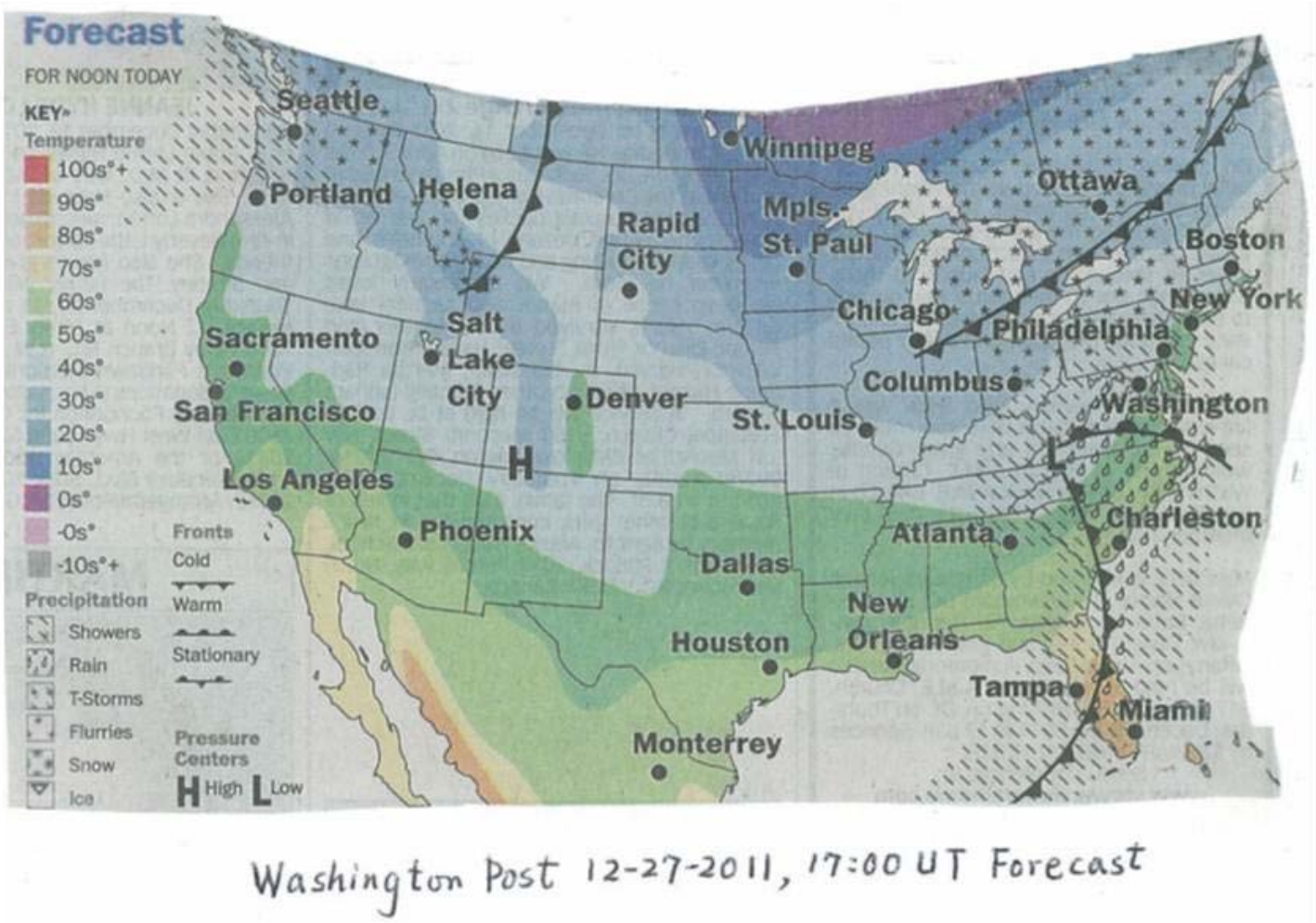

Washington Post 12-27-2011, 17:00 UT Forecast

The **Blizzard Storm** in USA Mid-West and ATMS Global **Emissivity Map**

Snow

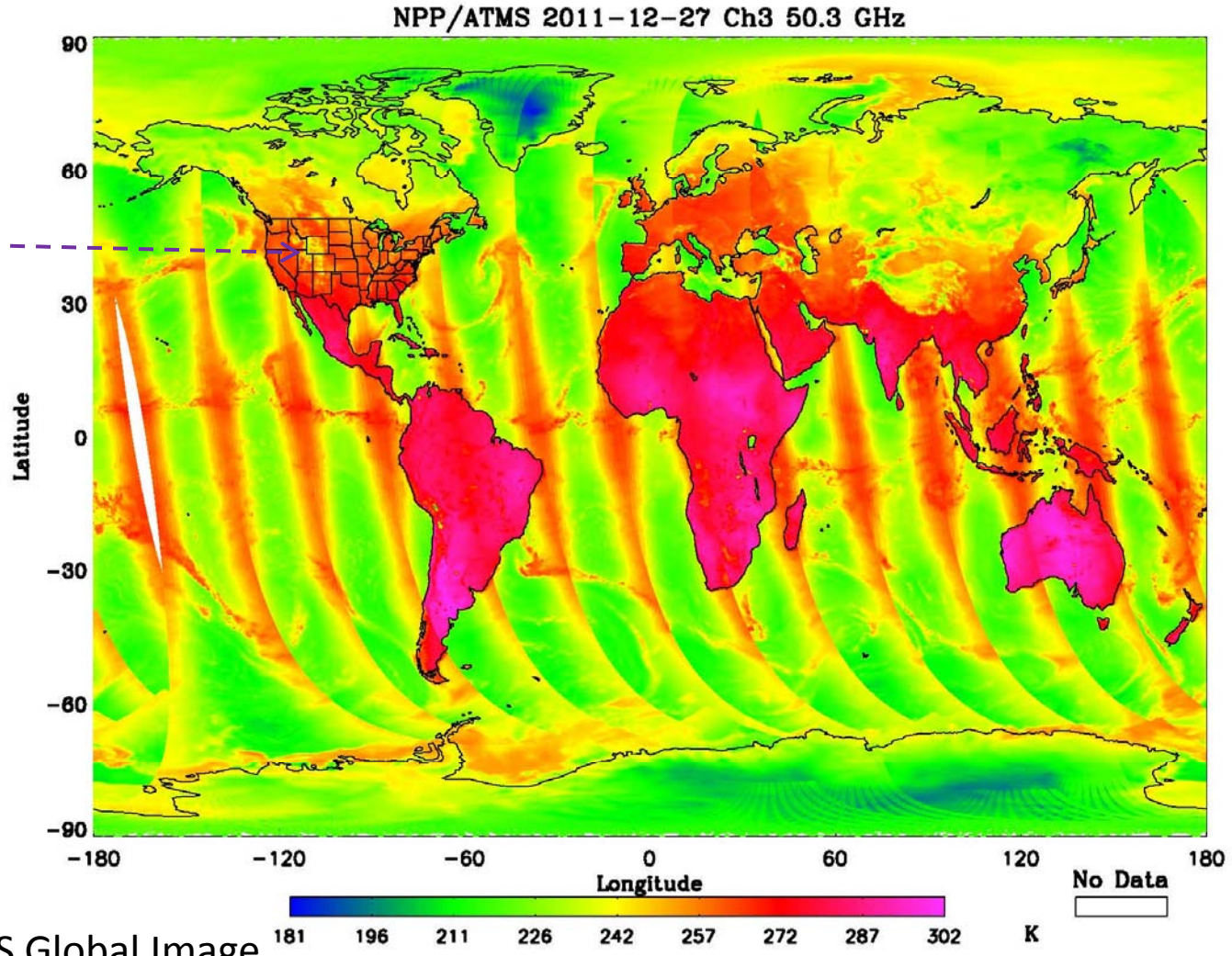

NASA ATMS Global Image

The emissivity of **land, ocean & ice** is different. See **sharp contrast** among them.

2. Functional Evaluation

2-1. Task #3 Objective

Evaluate that the sensor is operating as expected and was undamaged during the launch phase.

Responsible Teams: MITLL(S), NGES(Primary), **NASA**(S)

Exit Criteria:

A. Engineering telemetry's values are within acceptable limits.
B. Internal Target temperature sensors & video channels are working properly.
C. The **scan synchronization** agrees with radiometric data's time stamp.

Initial inspections of the sensor functional values are within acceptable limits. We still need further investigations of ATMS scan synch and time stamp issues. Specifically, we need to evaluate also the occasional ≈ **1ms glitch** in the CrIS RDR time stamp. Currently we **could improve** geolocation matching between ATMS/CrIS, compared to ATMS/CrIS 0 sec sync (no sync timing adjustment). Namely, **ATMS 47/CrIS 15 sync** would reduce the geolocation matching errors from 69.4" to 3.60", or 2.141 km to 0.111 km.

3. Optimal Space View Determination

3.1. **Task #4 Objective**

Determine which of the pre-determined space view angles have the least interference from the spacecraft or Earth intercept.

Responsible Teams: MITLL(Co-Primary), NOAA/STAR(CP), **NASA**(CP)

Exit Criteria:

Select the least obstructed space view profile among 4 SV sectors (SPs 1 – 4) centered at 6.66º, 8.33º, 10.0º & 13.33º (below NPP+Y axis).

3.2. Background

In ATMS scan lay-out, the scan pixel 97 (or **SV1**) is closer to **Earth limb**, the scan pixel 100 (or **SV4**) is closer to NPP **satellite platform**. We plan to show the performance of ATMS SPs 1 – 4 by analyzing SV1 and SV4 data count fluctuations, which would indicate potential impact resulting from any spacecraft or earth limb effects. **Neal Baker** speculated that **s/c** infringements or **earth limb** infringements might be on the order of a few tenths of Kelvin. We will evaluate this potential impact in this study. The **view geometry** of ATMS SPs and SVs 1 – 4 is shown in next page.

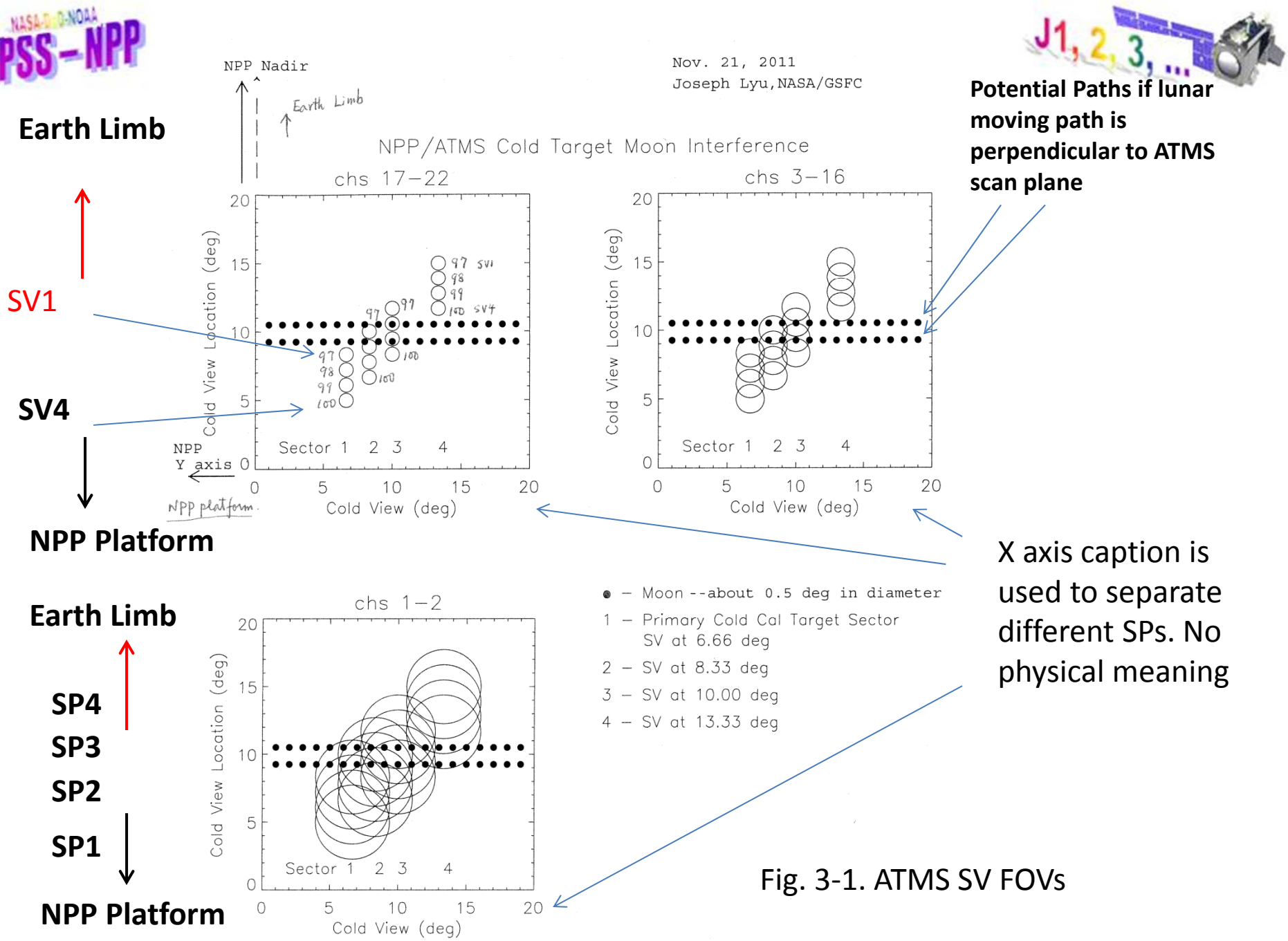

Fig. 3-1. ATMS SV FOVs

3.3. Our Methodology

a. Find **contiguous** (slightly longer than) **24 hours** time series (if applicable). We use SV1 & SV4, separately in this study.
b. Avoid lunar (or potential) contamination data regions.
c. Remove diurnal variation (or orbital variation).
d. (**Approach # 1**) Find mean, <n>, & standard deviation, σ, in the data & determine which SP may have less s/c &/or earth limb infringements.
e. (**Approach #2**) Use <SV1> – <SV4> to determine optimal SP, inspired by N. Baker.

Since the moon was in ATMS SV surroundings from **Dec. 3 to Dec. 6**, 2011, most of these data regions were not used in this study. For SP4, Dec. 3 data were not used. For SP1, (repeatability test) data from Dec. 3 to Dec. 6 (partial) were not used. Since our **main goal** is to assess the impact either from **s/c** and/or **earth limb infringements**, to implement performance evaluation, using **lunar un-affected** (at least not nearby) **data** sets is essential for these comparisons.

3.4. Results

We show some typical **plots** w/o diurnal variations in the following pages.

Nov. 18 SV1 Diurnal variation was removed SV1 Nov. 19

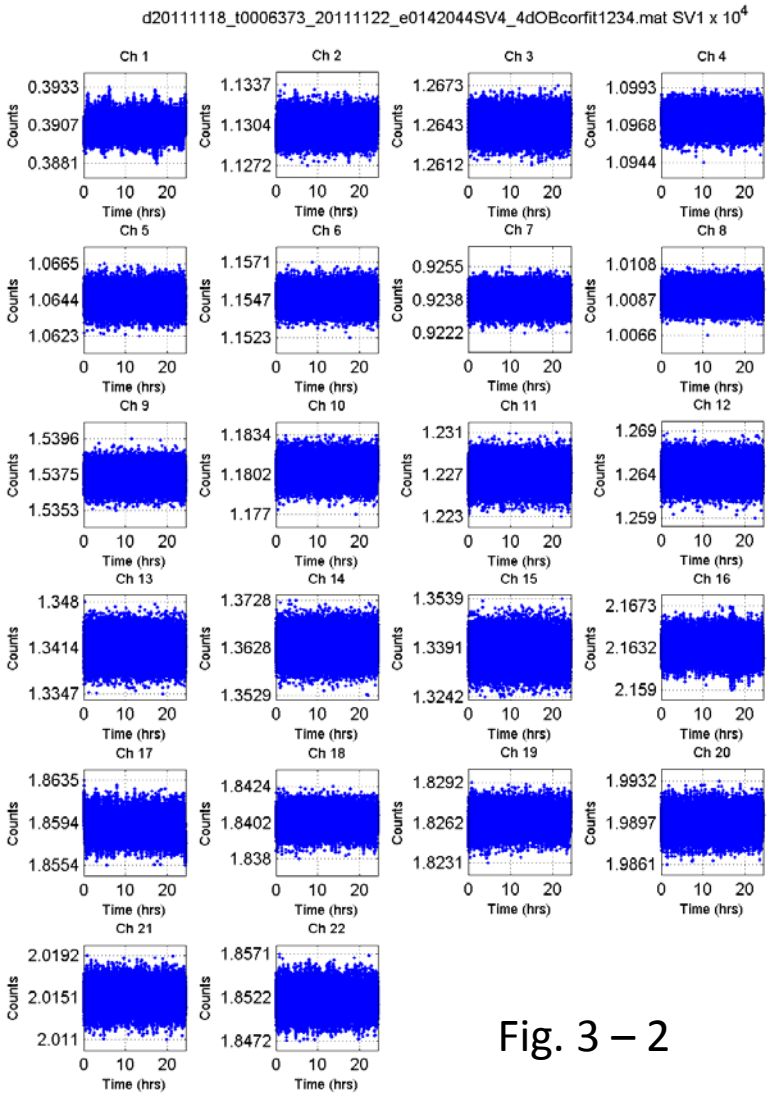

Fig. 3 – 2

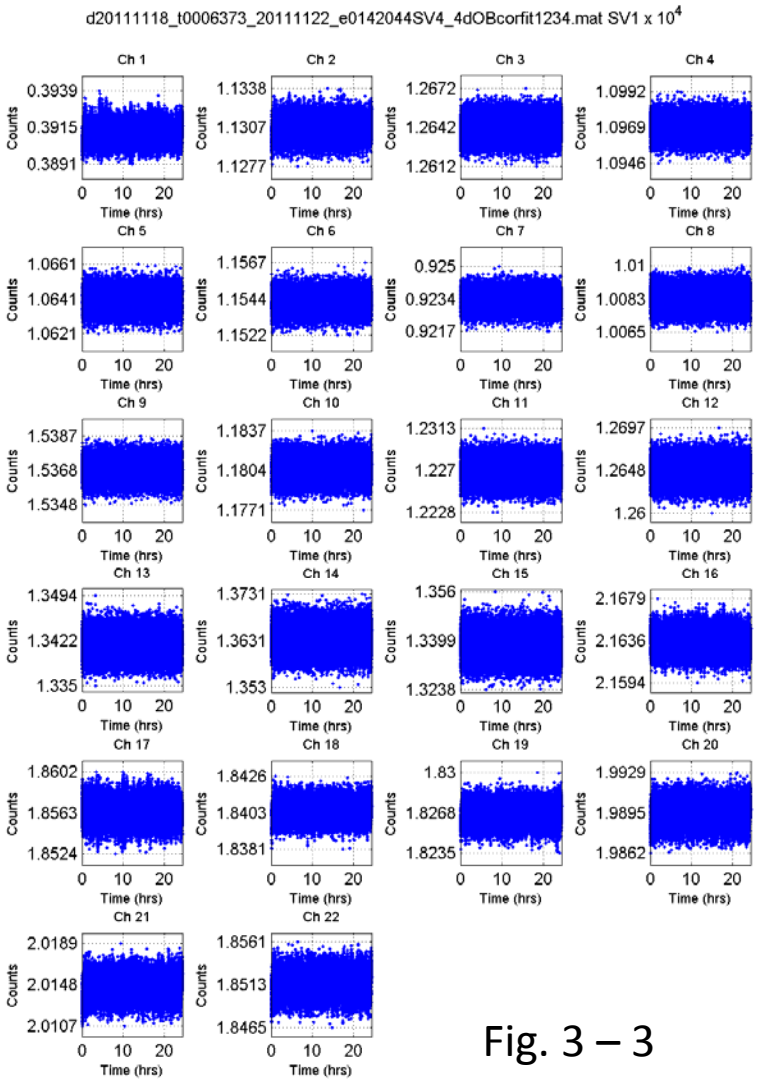

Fig. 3 – 3

Comparing two different 24 hours data sets, here shows SP1 repeatability result.
See later SP1 results for comparisons. SP1

Dec. 6-7 SV1 Diurnal variation was removed **SV4** Dec. 6-7

SP1

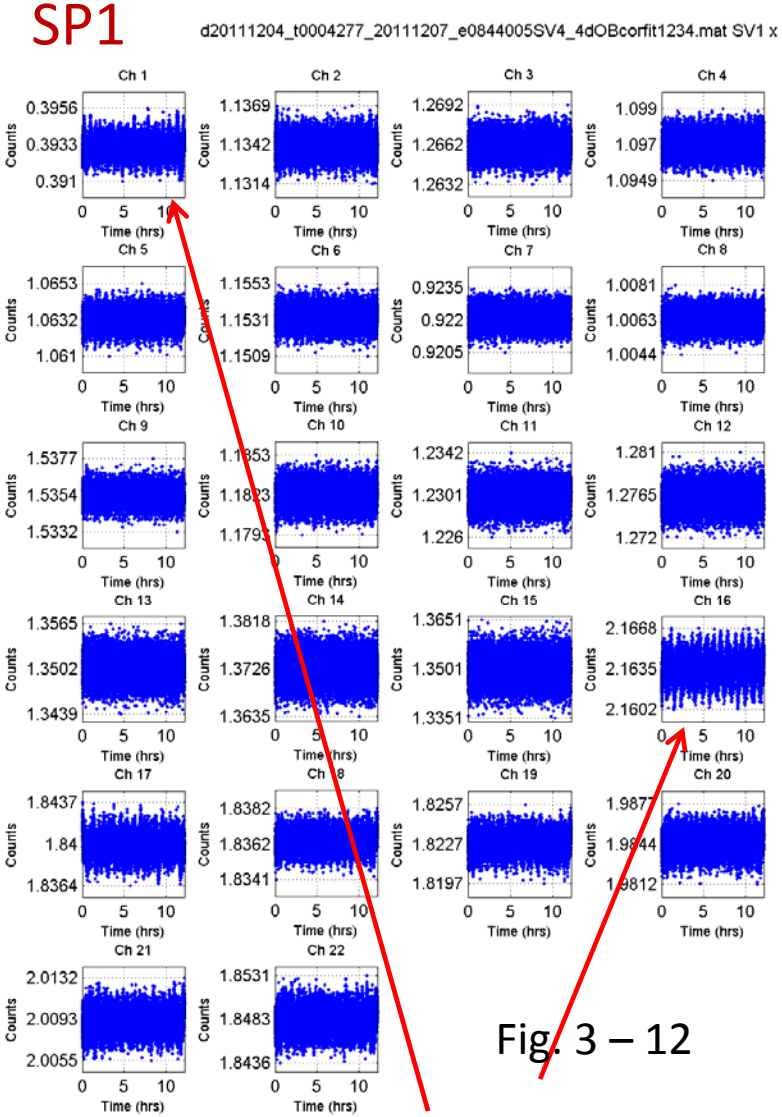

Fig. 3 – 12

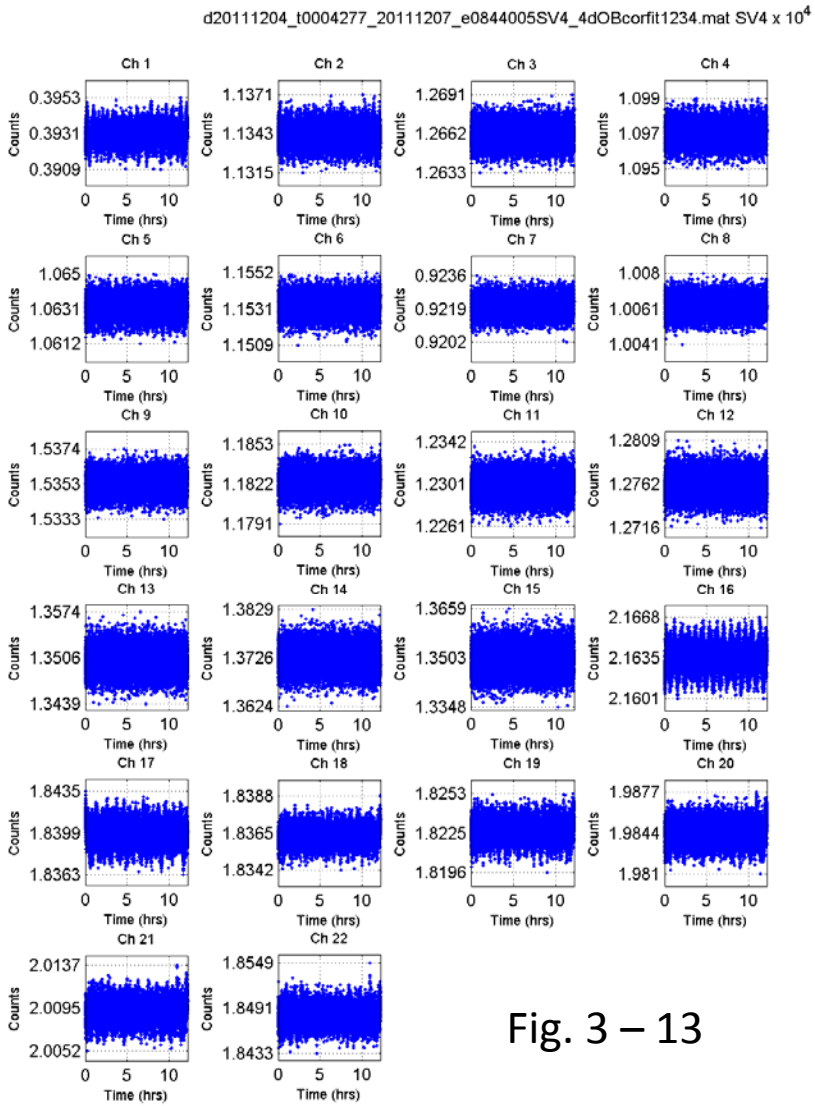

Fig. 3 – 13

Found also 50.5 min (half orbital) periodical noise component, associated with ATMS Shelf & RFE temperature variations (see Figs. 3 – 14 to 3 – 16).

Nov. 18 SP1 Dec. 8 SP1

> 24 hours RDR Count data > 6 hours data

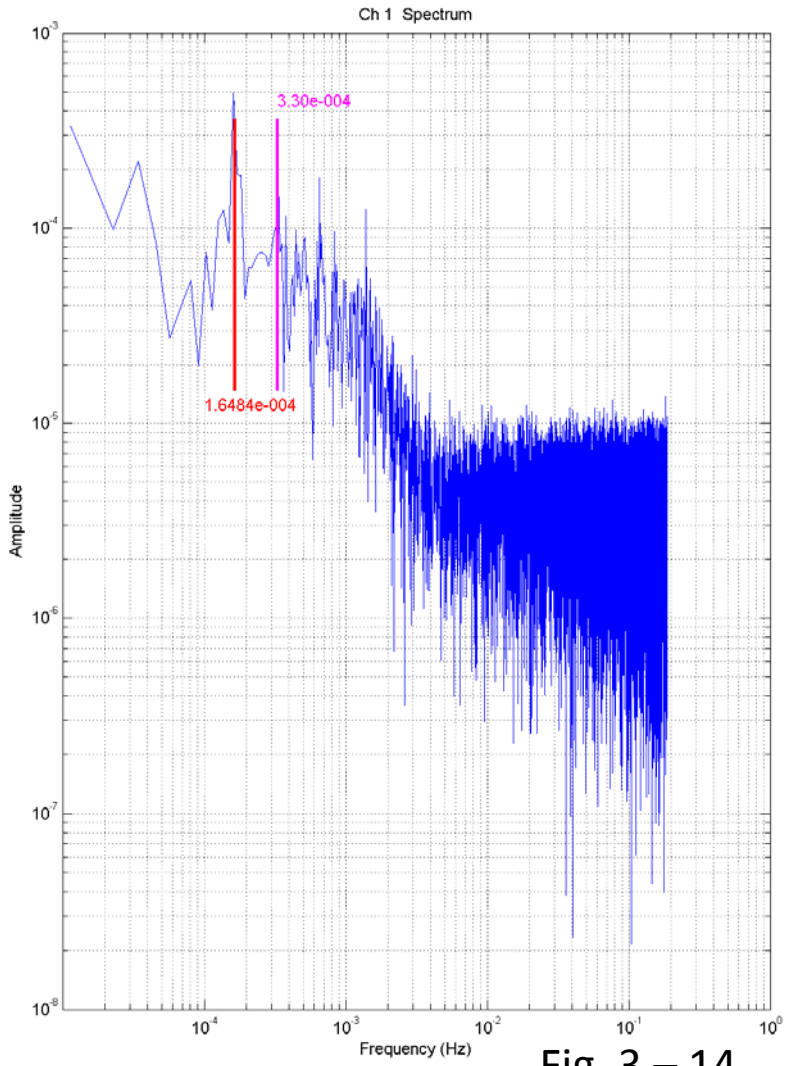

Fig. 3 – 14

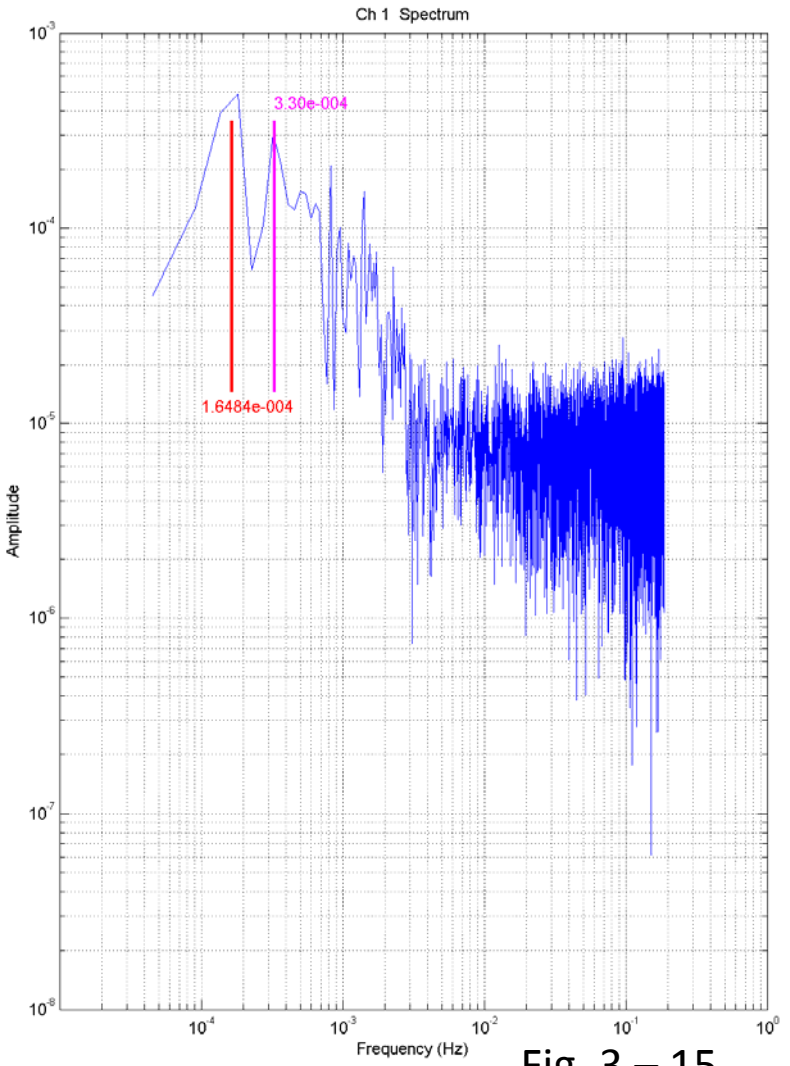

Fig. 3 – 15

Shown above are diurnal (removed in this study) & half orbital variation components

Derived from ATMS Housekeeping data.

Use Shelf Temperature

Dec. 8 SP1

> 6 hours data

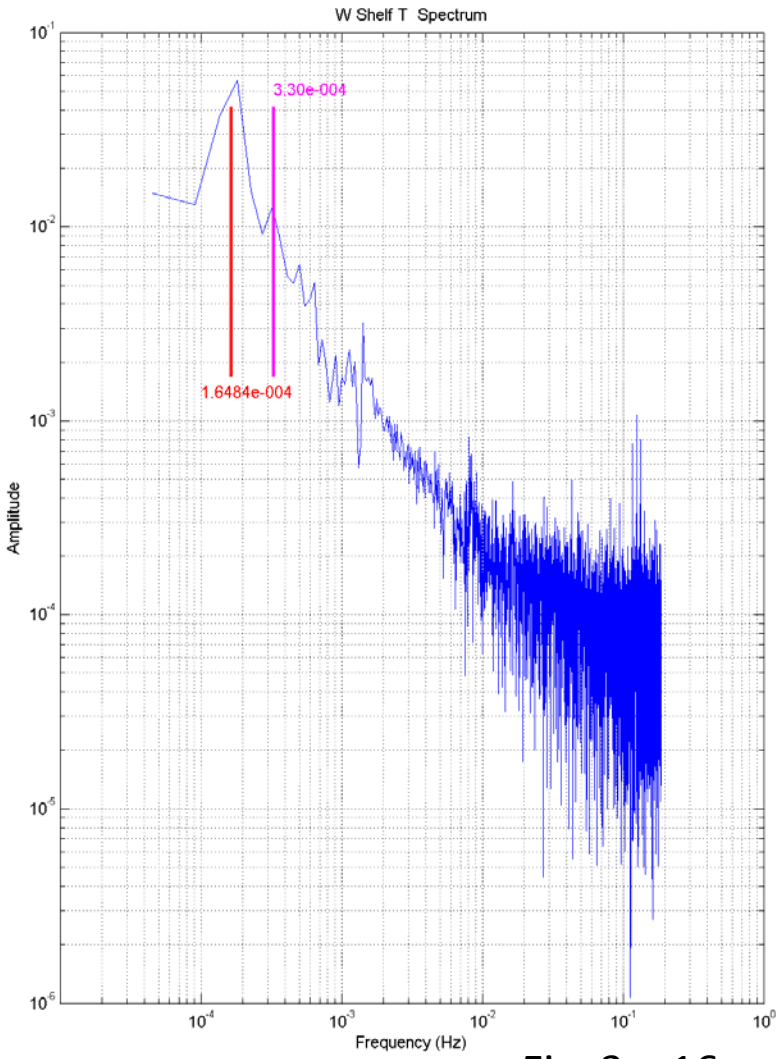

Fig. 3 – 16

3.5. Computed Results In Tables

Choose contiguous data section from the following dates to perform optimization analysis

SP1 – Nov. 18 – Nov. 19, 2011 (> 48 hrs, comparing two different 24 hours data sets, see tables 3-1 and 3-2, for repeatability result)

SP2 – Nov. 26 – Nov. 27, 2011 (> 48 hrs)

SP3 – Nov. 29 – Nov. 30, 2011 (> 24 hrs)

SP4 – Dec. 1 – Dec. 2, 2011 (> 21 hrs)

SP1 – Dec. 6/7 (> 12 hrs) & 8 (> 6 hours)

In tables 3-1 to 3-7, we have removed diurnal variations before analyzing data. Please note the magenta highlighted results for comparisons. See more repeatability analysis results in tables 3-6, 3-7, and 3-8. In table 3-8, we have removed also half orbital variation, an additional low frequency noise component.

SP1

Nov. 18 SV1			SV4	
Ch	<n>	σ	<n>	σ
1	3906.8,	6.1;	3906.0,	5.9
2	11303.1,	7.6;	11304.5,	7.5
3	12642.8,	7.6;	12643.1,	7.5
4	10972.0,	5.8;	10972.0,	5.8
5	10644.1,	5.3;	10644.2,	5.3
6	11548.0,	5.5;	11548.0,	5.5
7	9238.4,	4.1;	9237.9,	4.2
8	10089.5,	4.7;	10089.2,	4.7
9	15373.0,	5.2;	15372.7,	5.2
10	11805.4,	7.7;	11805.2,	7.7
11	12270.0,	10.1;	12269.6,	10.0
12	12642.6,	11.3;	12642.1,	11.5
13	13413.1,	16.8;	13412.9,	16.8
14	13632.9,	24.2;	13632.8,	24.2
15	13380.1,	38.2;	13379.4,	38.2
16	21633.0,	10.6;	21631.8,	10.3
17	18591.3,	9.8;	18590.6,	9.8
18	18403.4,	5.5;	18403.0,	5.5
19	18263.7,	7.4;	18263.2,	7.5
20	19896.8,	8.9;	19896.3,	9.0
21	20150.7,	10.4;	20150.3,	10.4
22	18519.0,	12.7;	18518.6,	12.6

Table. 3 – 1

Nov. 19 SV1			SV4	
Ch	<n>	σ	<n>	σ
1	3910.8,	5.9;	3910.0,	5.9
2	11306.2,	7.3;	11307.5,	7.3
3	12641.1,	7.5;	12641.5,	7.5
4	10969.7,	5.8;	10969.7,	5.7
5	10639.8,	5.2;	10639.9,	5.2
6	11542.5,	5.4;	11542.6,	5.4
7	9232.9,	4.1;	9232.4,	4.1
8	10082.6,	4.6;	10082.4,	4.6
9	15368.3,	5.1;	15367.9,	5.1
10	11805.0,	7.7;	11804.7,	7.8
11	12269.5,	10.1;	12269.2,	10.0
12	12647.4,	11.5;	12646.7,	11.4
13	13415.4,	16.8;	13415.2,	16.9
14	13635.2,	24.5;	13635.2,	24.4
15	13384.6,	38.3;	13384.7,	38.3
16	21635.2,	10.7;	21634.0,	10.5
17	18563.3,	9.8;	18562.6,	9.8
18	18404.7,	5.3;	18404.3,	5.3
19	18266.3,	7.4;	18265.8,	7.4
20	19894.6,	8.6;	19894.0,	8.6
21	20146.0,	10.0;	20145.5,	9.9
22	18514.1,	12.1;	18513.6,	12.0

Table. 3 – 2

SP2 Nov. 26 SV1 **SV4**

Ch	<n>	σ	<n>	σ
1	3923.1,	6.0;	3922.3,	6.0
2	11326.4,	7.4;	11326.3,	7.4
3	12648.9,	7.5;	12648.1,	7.5
4	10967.2,	5.8;	10966.4,	5.8
5	10629.6,	5.2;	10628.8,	5.3
6	11533.2,	5.5;	11532.0,	5.5
7	9224.1,	4.1;	9223.6,	4.2
8	10067.3,	4.7;	10066.7,	4.7
9	15360.6,	5.1;	15359.9,	5.2
10	11817.4,	7.8;	11816.8,	7.8
11	12287.6,	10.0;	12286.8,	10.0
12	12705.3,	11.5;	12704.6,	11.6
13	13460.7,	16.9;	13460.2,	16.9
14	13682.9,	24.4;	13682.3,	24.4
15	13443.5,	38.3;	13443.3,	38.1
16	21637.7,	10.6;	21635.6,	10.4
17	18436.5,	9.6;	18435.5,	9.5
18	18381.9,	5.3;	18381.3,	5.3
19	18236.1,	6.8;	18235.6,	6.8
20	19860.7,	8.7;	19860.0,	8.7
21	20110.5,	10.2;	20109.9,	10.1
22	18488.9,	12.4;	18488.3,	12.3

Table. 3 – 3

SP3 Nov. 29 SV1 **SV4**

Ch	<n>	σ	<n>	σ
1	3923.1,	6.2;	3920.4,	6.0
2	11342.5,	7.4;	11339.3,	7.3
3	12653.5,	7.5;	12652.0,	7.5
4	10966.9,	5.8;	10965.3,	5.8
5	10628.7,	5.2;	10627.3,	5.2
6	11531.3,	5.4;	11529.4,	5.4
7	9220.7,	4.1;	9219.6,	4.1
8	10061.9,	4.6;	10060.7,	4.7
9	15357.1,	5.1;	15356.1,	5.2
10	11819.9,	7.8;	11818.8,	7.8
11	12292.6,	10.1;	12292.0,	10.1
12	12725.7,	11.6;	12724.9,	11.7
13	13476.8,	17.0;	13475.5,	17.1
14	13699.4,	24.6;	13697.6,	24.6
15	13464.1,	38.7;	13462.3,	38.4
16	21635.7,	10.8;	21632.8,	10.4
17	18414.6,	9.6;	18414.3,	9.6
18	18373.3,	5.3;	18372.8,	5.4
19	18225.8,	6.7;	18225.4,	6.7
20	19850.1,	8.5;	19849.4,	8.5
21	20098.0,	10.1;	20097.4,	10.1
22	18480.2,	12.6;	18479.5,	12.7

Table. 3 – 4

Dec. 1 SV1 **SV4** SP4

Ch	<n>	σ	<n>	σ
1	3936.1,	6.7;	3931.9,	6.2
2	11339.6,	7.5;	11338.8,	7.4
3	12661.0,	7.6;	12657.2,	7.6
4	10972.7,	5.9;	10969.8,	5.8
5	10632.8,	5.3;	10629.5,	5.3
6	11532.9,	5.6;	11529.9,	5.5
7	9221.1,	4.2;	9218.9,	4.2
8	10061.8,	4.7;	10059.5,	4.6
9	15349.1,	5.2;	15346.8,	5.1
10	11821.1,	7.7;	11819.5,	7.7
11	12294.4,	10.1;	12292.8,	10.1
12	12743.2,	11.6;	12741.0,	11.6
13	13492.4,	17.1;	13490.5,	16.9
14	13715.1,	24.7;	13713.0,	24.5
15	13479.3,	38.9;	13477.0,	38.6
16	21637.7,	11.5;	21634.9,	11.1
17	18405.5,	9.8;	18404.5,	9.8
18	18370.1,	5.3;	18369.6,	5.3
19	18227.6,	6.6;	18227.1,	6.6
20	19847.0,	8.6;	19846.4,	8.6
21	20094.6,	10.1;	20094.1,	10.0
22	18479.2,	12.4;	18478.6,	12.4

Table. 3 – 5

SP1 Dec. 6-7 SV1 **SV4**

Ch	<n>	σ	<n>	σ
1	3931.4,	6.0;	3930.6,	5.9
2	11340.6,	7.4;	11341.9,	7.3
3	12660.8,	7.5;	12661.0,	7.4
4	10970.5,	5.6;	10970.5,	5.7
5	10631.8,	5.1;	10631.9,	5.1
6	11532.8,	5.4;	11532.9,	5.5
7	9220.9,	4.1;	9220.5,	4.1
8	10063.0,	4.6;	10062.7,	4.7
9	15353.7,	5.1;	15353.4,	5.2
10	11823.5,	7.8;	11823.3,	7.8
11	12299.7,	10.0;	12299.3,	10.1
12	12761.7,	11.6;	12761.3,	11.7
13	13502.7,	16.9;	13502.6,	17.2
14	13725.9,	24.7;	13725.6,	24.4
15	13499.9,	38.7;	13499.9,	38.8
16	21635.7,	10.2;	21634.7,	10.0
17	18398.9,	9.5;	18398.2,	9.4
18	18363.4,	5.3;	18363.0,	5.4
19	18227.7,	7.3;	18227.2,	7.3
20	19844.8,	8.6;	19844.2,	8.5
21	20091.4,	10.0;	20091.0,	9.9
22	18481.4,	12.4;	18480.7,	12.3

Table. 3 – 6

Ch	Nov.18 SP1 SV1–SV4	Ch	Nov.19 SP1 SV1–SV4	Ch	Nov.26 SP2 SV1–SV4	Ch	Nov.29 SP3 SV1–SV4	Ch	Dec.01 SP4 SV1–SV4	Ch	Dec.08 SP1 SV1–SV4
1	0.7724,	1	0.8264,	1	0.8121,	1	2.6745,	1	4.1944,	1	0.7273,
2	-1.4121,	2	-1.3358,	2	0.1252,	2	3.1863,	2	0.8413,	2	-1.3329,
3	-0.2548,	3	-0.3658,	3	0.7885,	3	1.5664,	3	3.8034,	3	-0.3220,
4	-0.0013,	4	-0.0315,	4	0.7652,	4	1.6657,	4	2.8241,	4	-0.0206,
5	-0.1313,	5	-0.1253,	5	0.7538,	5	1.3676,	5	3.2664,	5	-0.1926,
6	-0.0350,	6	-0.0809,	6	1.1815,	6	1.8497,	6	2.9125,	6	-0.0315,
7	0.4565,	7	0.4367,	7	0.5334,	7	1.0276,	7	2.2107,	7	0.4627,
8	0.3094	8	0.2613	8	0.6483	8	1.1909	8	2.3242,	8	0.3255,
9	0.3656,	9	0.3207,	9	0.7114,	9	0.9949,	9	2.2981,	9	0.3026,
10	0.2314,	10	0.3232,	10	0.5802,	10	1.1091,	10	1.5827,	10	0.3105,
11	0.4032,	11	0.3581,	11	0.8452,	11	0.6654,	11	1.5395,	11	0.2707,
12	0.4867,	12	0.6911,	12	0.7505,	12	0.8212,	12	2.2192,	12	0.5667,
13	0.1906,	13	0.1545,	13	0.4322,	13	1.3887,	13	1.8793,	13	0.2103,
14	0.1195,	14	0.0127,	14	0.5471,	14	1.7881,	14	2.1112,	14	0.1864,
15	0.6899,	15	-0.1524,	15	0.1815,	15	1.7621,	15	2.2885,	15	-0.1207,
16	1.1850	16	1.1668	16	2.0394	16	2.8477	16	2.7686,	16	1.1416,
17	0.7276,	17	0.6763,	17	0.9346,	17	0.3595,	17	1.0205,	17	0.7151,
18	0.4006,	18	0.3695,	18	0.5457,	18	0.5549,	18	0.4847,	18	0.3652,
19	0.4747,	19	0.4266,	19	0.5525,	19	0.4809,	19	0.5388,	19	0.3977,
20	0.5803,	20	0.6007,	20	0.7551,	20	0.6847,	20	0.5873,	20	0.5604,
21	0.4715,	21	0.4889,	21	0.6087,	21	0.5856,	21	0.4893,	21	0.5316,
22	0.4017	22	0.4848	22	0.6347	22	0.6386	22	0.5934	22	0.4535

Table. 3 – 9, **SV1 – SV4** after removing diurnal variations

3.5. Concluding Remarks About Optimal SP

A. MIT-LL 's (Leslie, 12/7/2011) study of optimal SV from on-orbit data concluded that **if finding with no preferences, the SP1 should be optimal SP**. The rationales are: (1) **CATR patterns** were measured at **SVS1** (= **SP1**). (2) **Even** though the data analysis was **inconclusive**, it can be assumed that moving toward the Earth's limb **SVS2, SVS3, or SVS4 potentially risks having more sidelobes contaminated**. The criticism of choosing SVS1 is that the s/c contamination could be higher, but the estimated contribution (in the NGES error analysis from the PFM Cal. Data Book Table 9.2) that used the antenna pattern measurements was much lower from the S/C than the Earth (except the K and Ka channels which were comparable).

B. Compared among the magenta highlight lines in tables 3-1 to 3-5, we find that SP1 could be the optimal SP (**Approach #1**). There are two reasons:
(1). The mean count difference among SPs 1 & 4 for Chs 1 & 2 could be about > 30 counts (0.3 to 1%, not just a few counts for other channels) for staring at the same cold space. The SP1 may show the lowest mean count, see table 3-1 and 3-2.
(2). The FOV of Chs 1 & 2 is about 5.2 deg. It is more susceptible to the surrounding s/c and earth limb infringements than other channels. Chs 1 & 2 in SP1 shows the potential lowest mean counts.

C. On the other hand, based on our **Approach #1**, from SP1 repeatability tests, the results on Dec. 7 and Dec. 8 in tables 3-6 to 3-8, did not show similar low counts to those found on Nov. 18 and Nov. 19. This could imply that all SPs 1 – 4 have very similar (or no) response to either s/c or earth limb infringements. We find that **sensor electronic temperature drifting versus time is most probably one key factor that affects the SV performance** and **this approach** makes the evaluation of the optimal SPs somewhat **difficult**.

D. Nevertheless, our **2nd Approach** (#**2**) is to evaluate the **difference of SV1 and SV4 in the same SP**, with the same sensor temperatures. There would be **no temperature-dependent count drifting issues**. As noted in our Introduction, the scan pixel 97 (or SV1) is closer to Earth limb, and the scan pixel 100 (or SV4) is closer to NPP platform. The difference of SV1 and SV4, i.e., SV1 – SV4, from SPs 1 – 4 should provide us with a **good gauge to determine which SP would be the optimal SP** (thanks to **Neal Baker** for enlightening us, indirectly, with this approach). Regarding the infringements either from s/c or earth limb, we do find significant differences in SV1 – SV4 . The results of **SV1 – SV4 from SP1 and its repeatability tests show mostly and significantly the lowest counts** (see Table 3-9 for comparisons) . Thus, we conclude that among SPs 1 – 4, the SV pixels from SP1 have the lowest impact from either s/c or earth limb infringements.

E. Based on the Approach #2, moreover, the **repeatability tests** show relatively **consistent results** for SP1 (see 3 SP1 computed columns/results in Table 3-9).

F. In this study, the SV measurements from SPs 1 – 4 show very stable results and their SV performances are quite comparable. However, **all the evidences from our analysis indicate that SP1 is the optimal SP**. This SP1 should be used to optimize the analysis of ATMS on-orbit sensor performance.

4. Scan Angle

4.1. **Task #8 Objective**

Verify that the reflector's scan position in the science data packet matches the expected scan position.

Responsible Teams: NGES(Primary), MITLL(S), **NASA**(S)

Exit Criteria:

The reflector resolver counts are within two counts of their ground measurements and the scan positions are repeatable.

We don't have enough time to prepare for this report. We would **postpone this task** until next review meeting. However, our **initial inspections** of scan angle performance indicates that ATMS on-orbit reflector resolver counts are within the acceptable ranges.

5. Radiometric Sensitivity

5.1. **Task #9 Objective**

Evaluate the on-orbit radiometric sensitivity (NEΔT).

Responsible Teams: NGES(Primary), MITLL(S), **NASA**(S), NOAA/STAR(S)

Exit Criteria:

On-orbit measurements of NEΔT are lower than the requirements and any deviations from ground measurements are investigated and recorded.

We don't have enough time to prepare for this report. We would **postpone this task** until next review meeting. However, our **initial inspections** of NEΔT indicates that on-orbit radiometric sensitivity meets the specification.

6. Lunar Intrusion Mitigation

6.1. **Task #14 Objective**

Determine a routine procedure for dealing with lunar contamination of the cold space calibration target.

Responsible Teams: NASA(Co-Primary), NOAA/STAR(CP)

Exit Criteria:

A lunar contamination mitigation plan is prepared and executed.

6.2. Background

For one potential **worst lunar intrusion case**, one on Dec. 5, 2011, at 6:41, we find that **all 4** SV pixels got contaminated for K/Ka bands, and **only 1** SV pixel was free of lunar contamination for V, W and G bands. If we adopt **current** (NG established) **plan** to abolish SDR/TDR processing when we have less than 3 SV pixels free of lunar contamination, then at 6:41 we would lose about 25 min for K/Ka bands (Chs 1 & 2) data and lose about 7 – 12 min worth of data for all other bands. Then from Dec. 3 to Dec. 5, 2011, we would **lose**, at most, about **10 hours** worth of TDR, calibrated SDR, Re-map SDR, and EDR data products during this time. Some lunar contaminated data are presented in the following pages.

Fig. 6-1. Lunar Intrusion to SV from Dec. 4 to Dec. 5, 2011

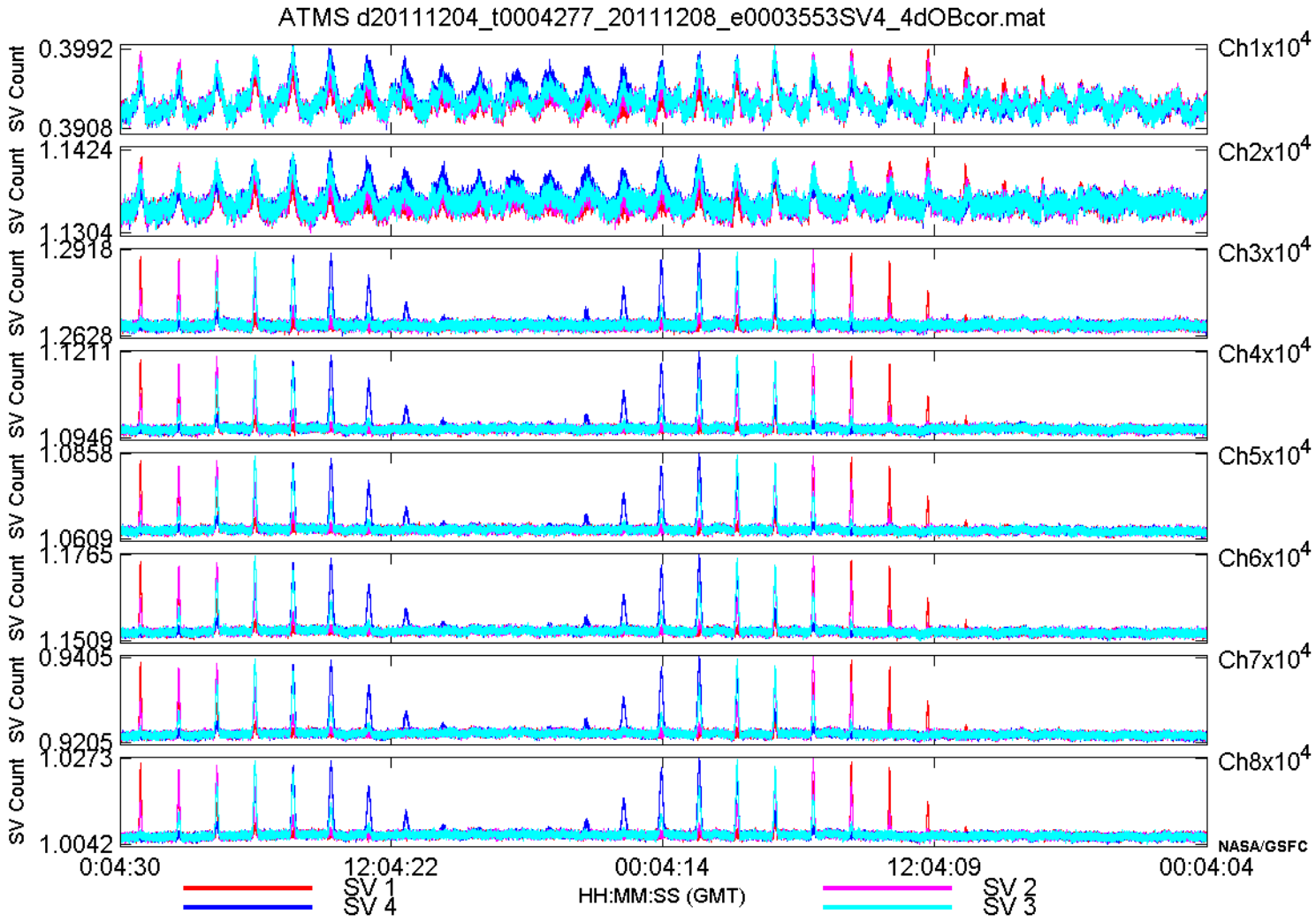

Fig. 6-2. Lunar Intrusion to SV from Dec. 4 to Dec. 5, 2011

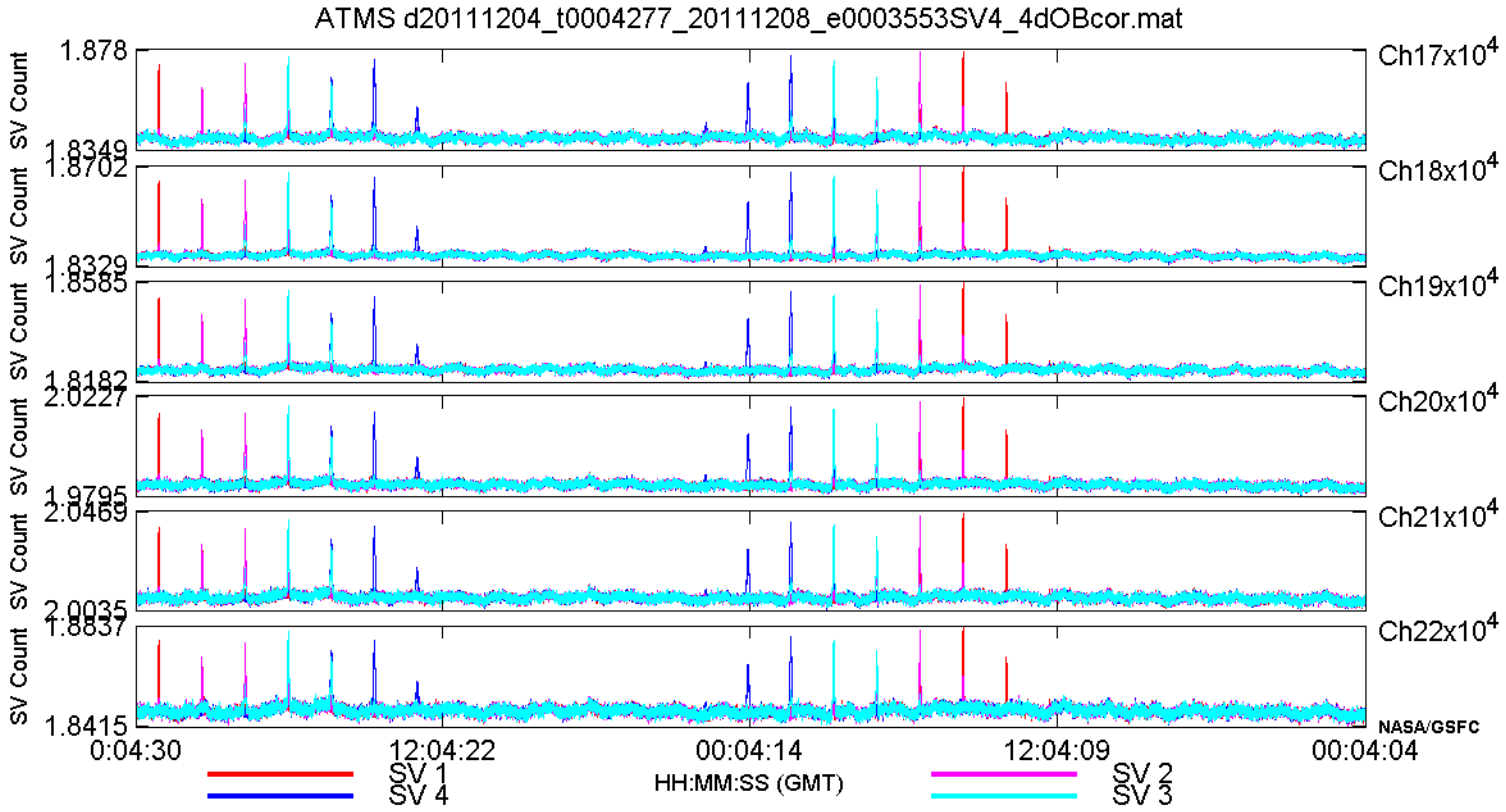

Fig. 6-3. Lunar Intrusion to SV on Dec. 5, 2011 centered at 06:41:15

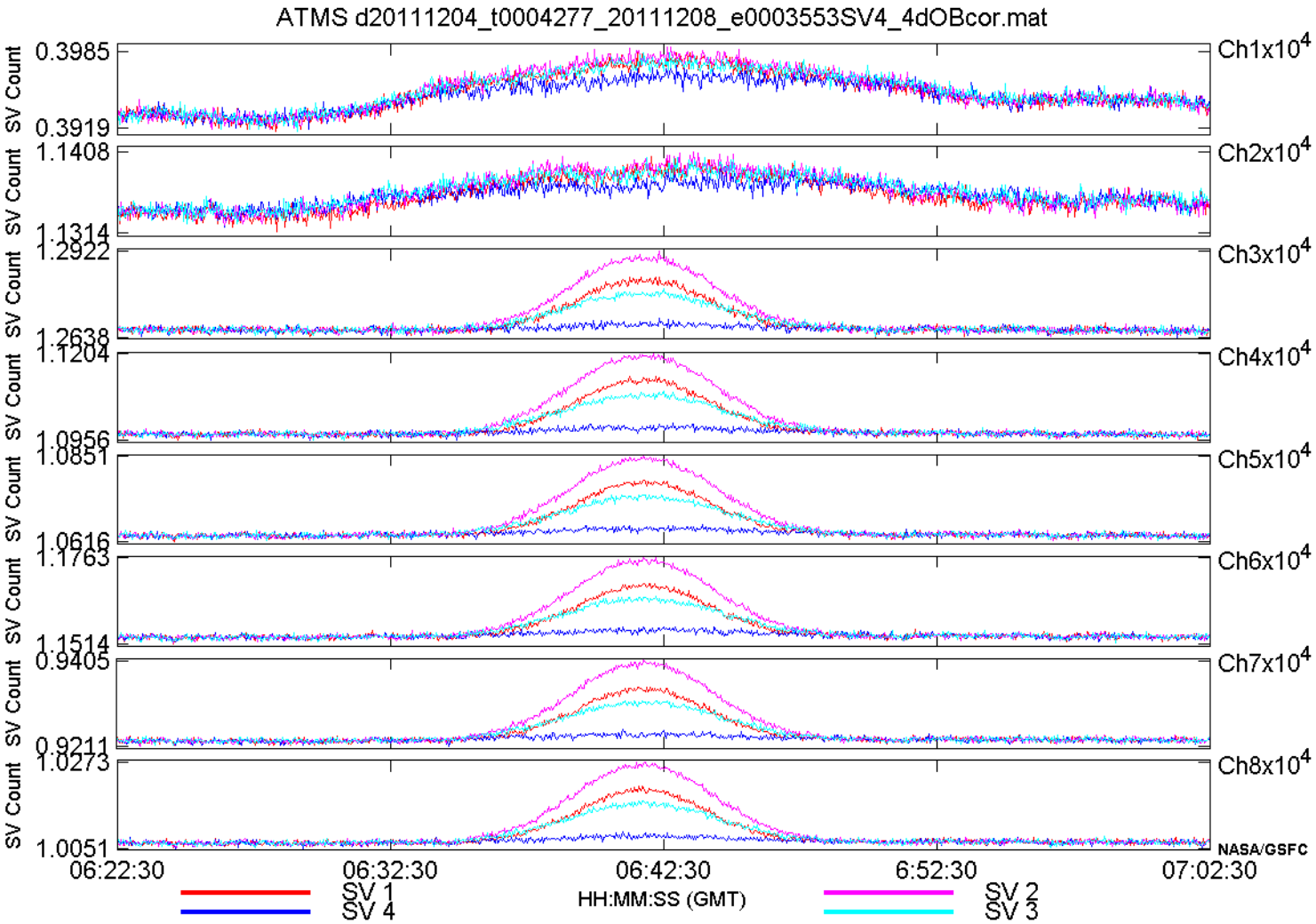

Lunar ϕ = -57.48°, moon center is ≈ 0.15° from SV2 FOV center

For K/Ka bands, NO good SV. For V/W bands, SV4 is good for data processing.

The worst lunar contamination lasted for about 25 min, for K/Ka bands.

Fig. 6-4. Lunar Intrusion to SV on Dec. 5, 2011 centered at 06:41:15

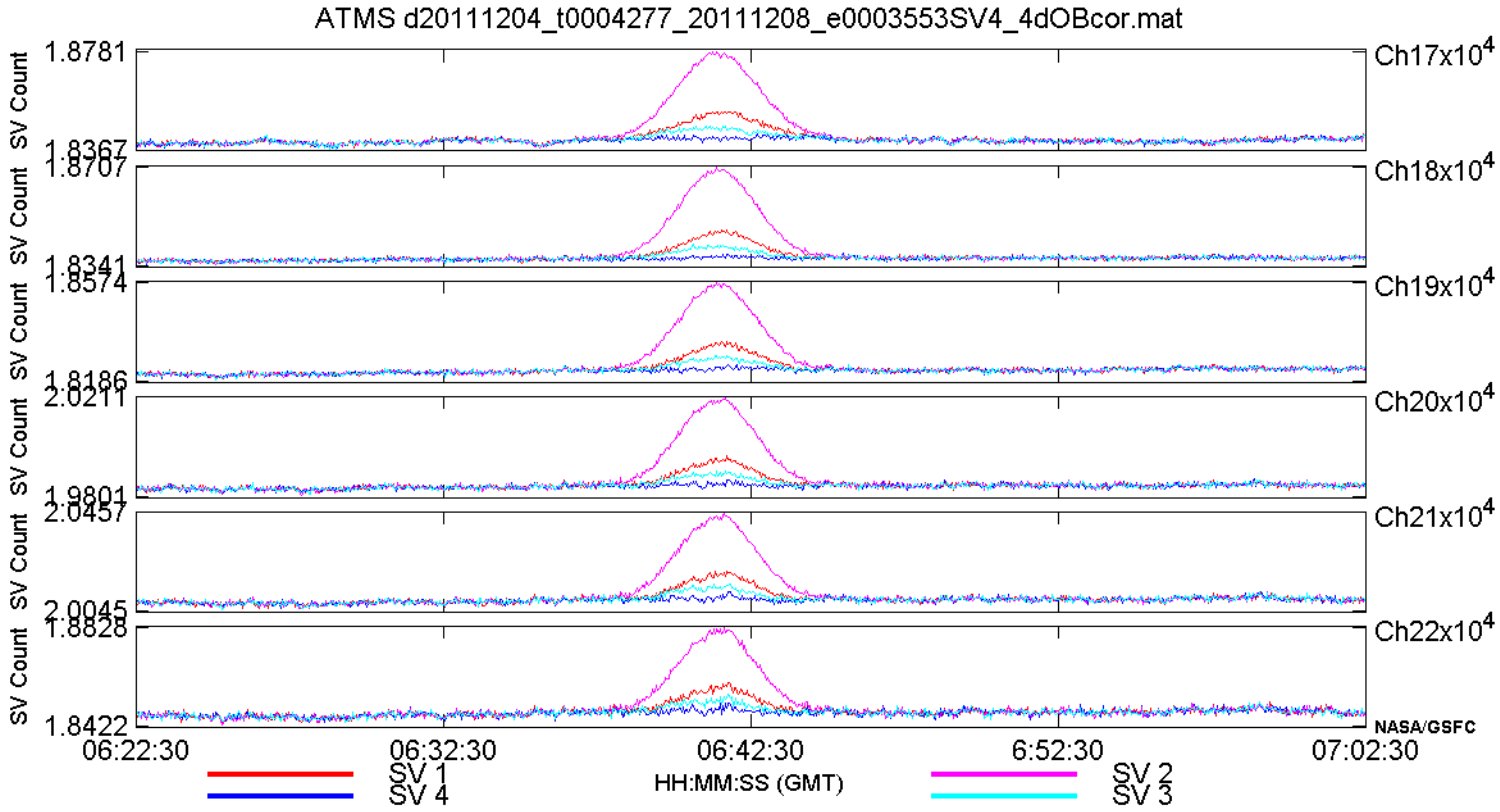

Lunar ϕ = -57.48°, moon center is ≈ 0.15° from SV2 FOV center

For G bands, SV4 is good for data processing. For V/W/G bands, the worst lunar contamination lasted for about 7 – 12 min.

Use **slide # 8** to explain about one potential lunar intrusion mitigation plan

Fig. 6-5. Lunar Intrusion to SV from Jan. 2 to Jan. 3, 2012

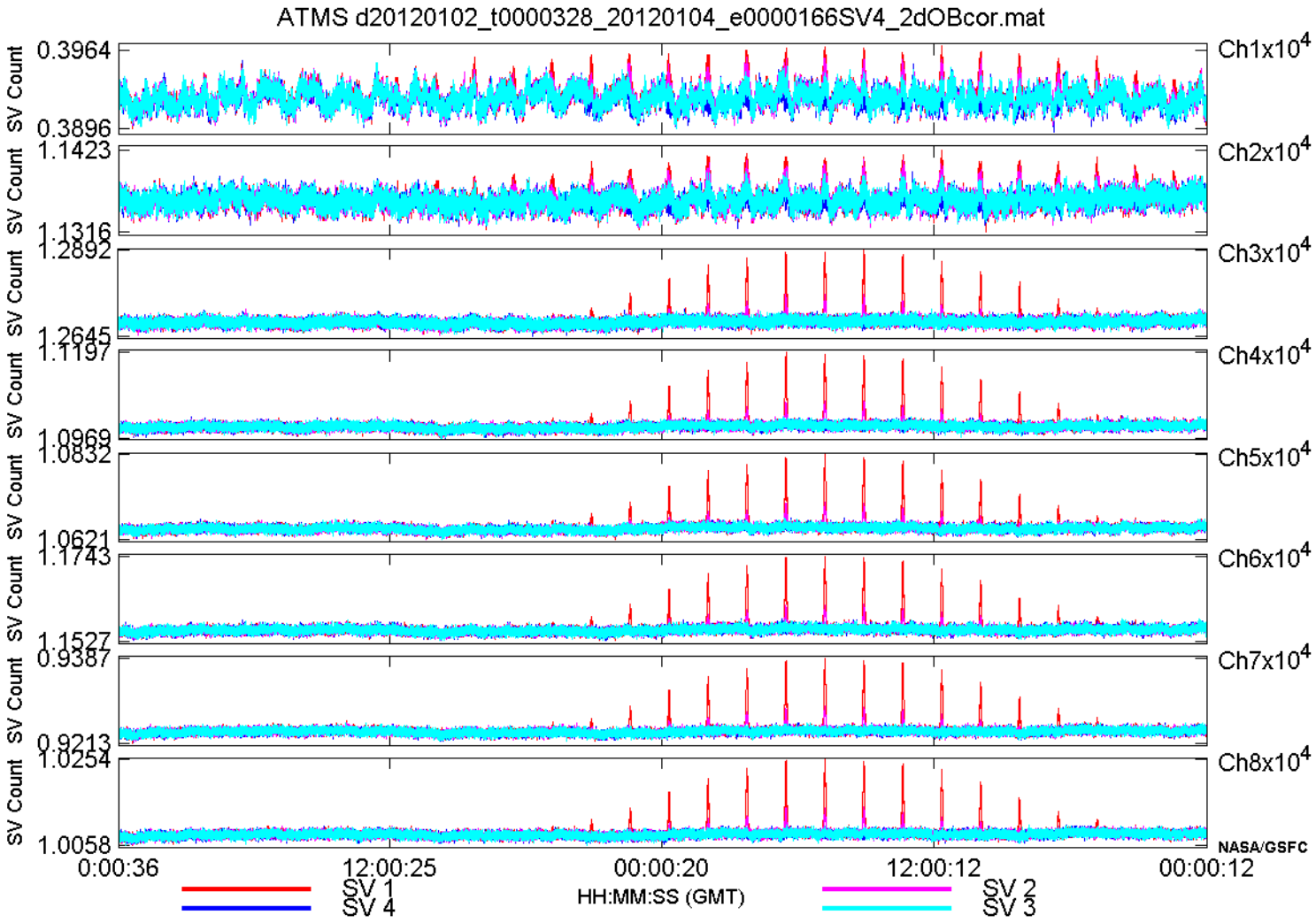

Fig. 6-6. Lunar Intrusion to SV on Jan. 3, 2012 centered at 08:53:12

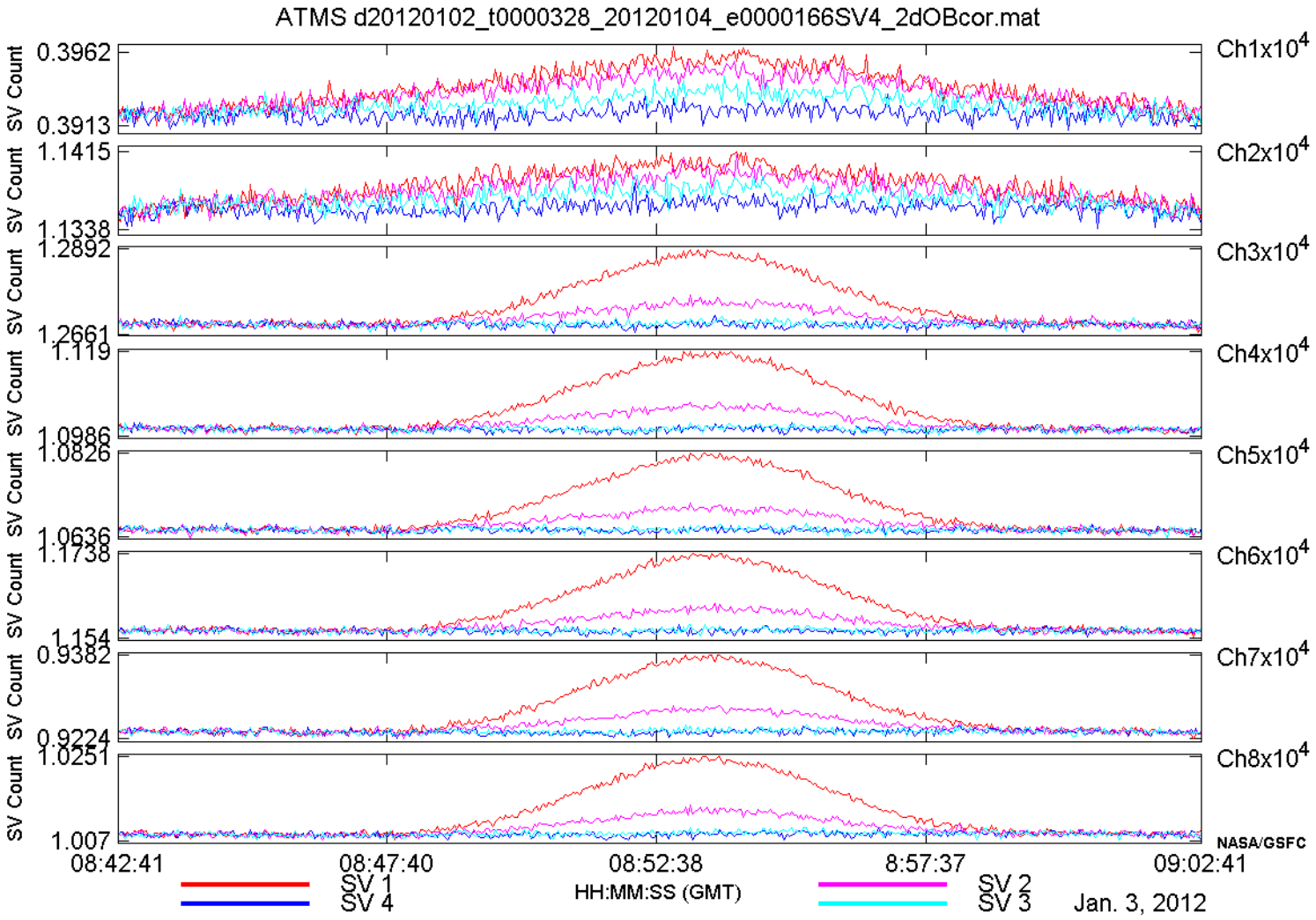

Lunar ϕ = -66.95°, moon center is ≈ 0.55° from SV1 FOV center

For K/Ka bands, SV4 is good. For V/W bands, two SVs, SV3 & SV4, are good .

Fig. 6-7. Lunar Intrusion to SV on Jan. 3, 2012 centered at 08:53:12

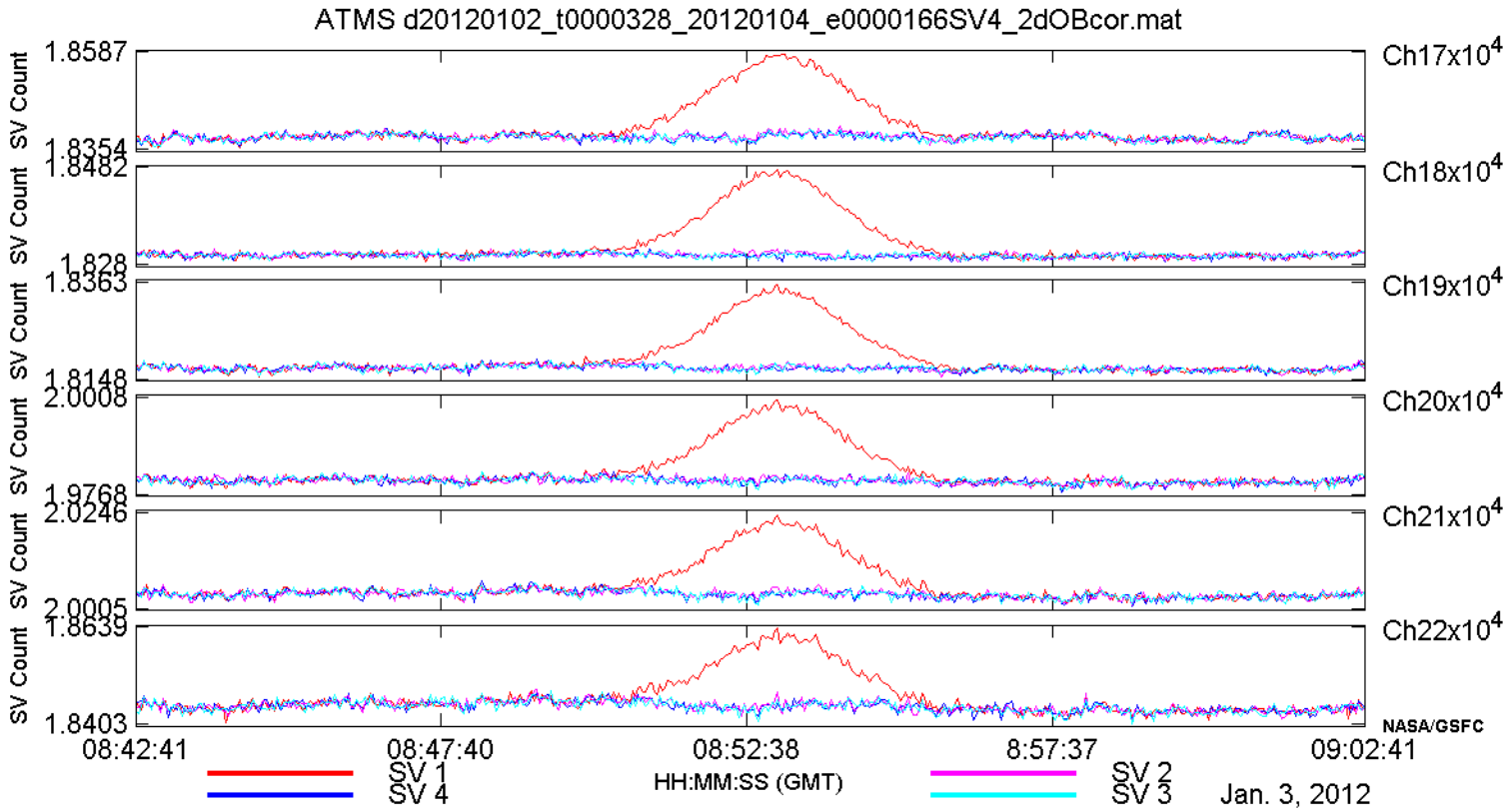

Lunar ϕ = -66.95°, moon center is ≈ 0.55° from SV1 FOV center

For G bands, three SVs, SV2, SV3 and SV4 are good for data processing.

Fig. 6-8. Lunar Intrusion to SV on Jan. 3, 2012 centered at 22:35:41

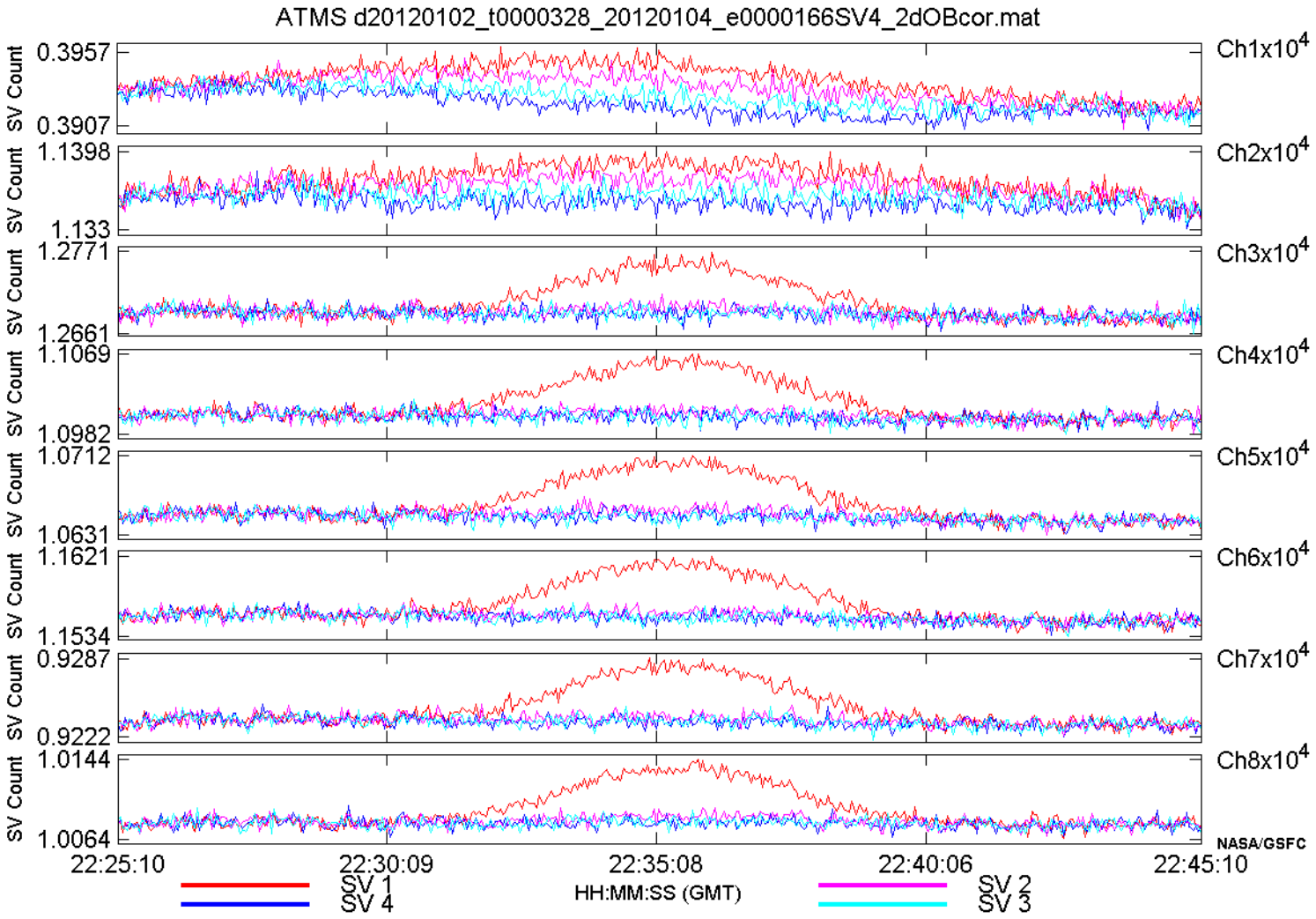

Lunar ϕ = -60.19°, moon center is ≈ 3.04° from SV1 FOV center

For K/Ka bands, SV4 is good. For V/W, three SVs are good. For G, all SVs are good.

6.3. Solutions And Recommendations

There are **two proposed methods** of lunar intrusion mitigation:

1) We simply ignore pixels that are corrupted by the moon, but we adopt at least one (if applicable) of the four available pixels is unaffected, **and**
2) We correct for the lunar perturbation using the viewing geometry and a radiometric model of the moon, **or**
3) We just use "Good" pixels (even one or their average, if applicable) to substitute for the mean SV in the current data processing codes.

As an alternative (**3rd method**), processing system needs to be able to bridge across samples where no calibration can be done due to rejected cold-cal (SV) views. Namely, we can use a lunar radiative model and use it to correct contaminated SVs. On **Aqua**, the "**bridge across gaps**" method is adopted. The gain should be stable enough to allow that, but we need to assess and confirm the stability status of the gain.

7. EV Contamination Mitigation

7.1. (Potential) **Task #26 Objective**

(Note: In the NPP/ATMS OPSCON, there are only 25 assigned tasks)
Determine a routine procedure for dealing with Deep Space (DS) contamination in the EV target (pixels).
Responsible Teams: NASA(Co-Primary), All Other Teams (CP)
Exit Criteria:
A deep space (DS) contamination mitigation plan is prepared and executed.

7.2. Background

VIIRS lunar maneuver is scheduled to perform (almost) monthly with lunar ϕ of 55 degrees, within 4 orbits. One potential (possibly 2nd) worst deep space intrusion case would happen on Nov. 23, 2012, at 11:09:32 UTC, which VIIRS would perform -14.1411 deg roll. (The worst one could happen on 12/5/2011, a -14.9275 deg roll, cancelled.) This would cause up to 9 pixels of ATMS EV to view deep space (DS).

For VIIRS lunar maneuver, the roll angle would be maintained for 4 min each time, centered on the point in the orbit where the NPP-to-Moon vector is in the NPP Y-Z plane on the daylight side of the orbit.

Table 7-1. Projected VIIRS Maneuver Roll Angle/Time Table, developed by Junqiang Sun at MCST/NICST/NICSE

M/ D/ Y	H: M: S	Rol_ang	SMnVr	Latitude	E_side
12/5/2011	11:44:54	-14.9275	55.2	-13.98	D
1/4/2012	8:48:58	-9.7232	55.42	-50.4	D
2/3/2012	6:03:35	-5.3438	55.39	-50.11	D
3/3/2012	23:58:40	-5.6433	55.71	-37.79	D
4/2/2012	14:34:47	-8.5507	55.71	-11.36	D
5/2/2012	1:52:09	-8.3914	55.55	30.07	D
5/31/2012	9:43:05	-2.7864	55.87	59.11	D
10/24/2012	22:31:32	-6.2618	55.37	49.43	D
11/23/2012	11:09:32	-14.1411	55.62	17.93	D
12/23/2012	4:45:26	-12.8873	55.55	-36.8	D

In fact, the first VIIRS Lunar maneuver was performed on 1/4/2012 with a roll angle of -9.488 deg: Start 08:43:53, End 08:46:53. Dwell for 4 min & Return to Nadir: Start 08:50:53, End 08:55:53. The whole VIIRS lunar maneuver lasted for ≈ **12 min**. We present ATMS EV contamination analysis in the following pages.

ATMS scans off Earth limb while VIIRS performs 1/4/2012 lunar roll maneuver.
For the K/Ka bands, ≈ 5.2 deg FOV, there are 3 EV pixels with DS contamination.
For the V bands, ≈ 2.2 deg FOV, there are 3 EV pixels with DS contamination.

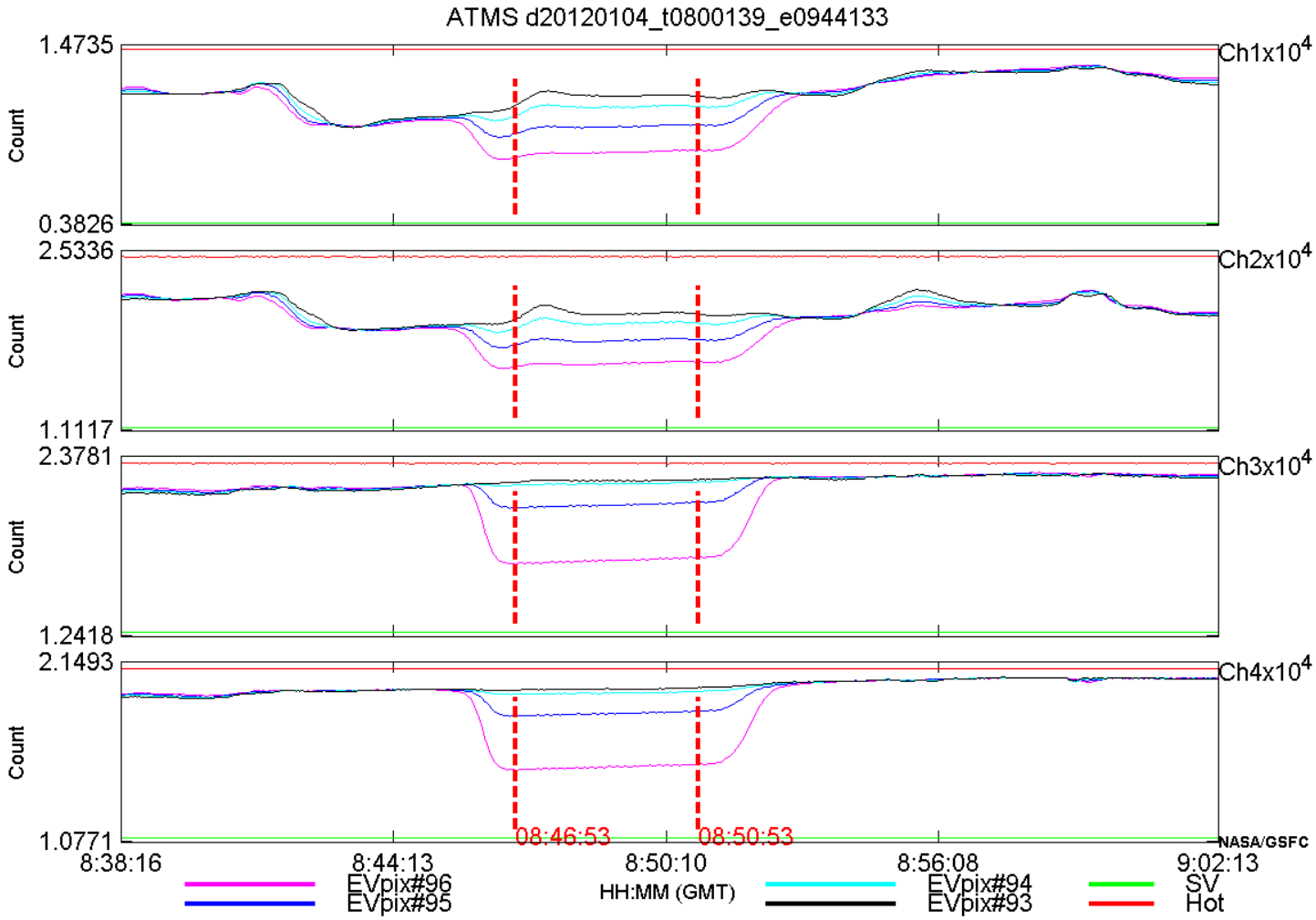

Fig. 7-1. Impacts to ATMS K/Ka, V/W bands from VIIRS -9.5 deg Lunar Roll.

ATMS scans off Earth limb while VIIRS performs 1/4/2012 lunar roll maneuver.
For the G bands, ≈ 1.1 deg FOV, there is 1 EV pixel with DS contamination.

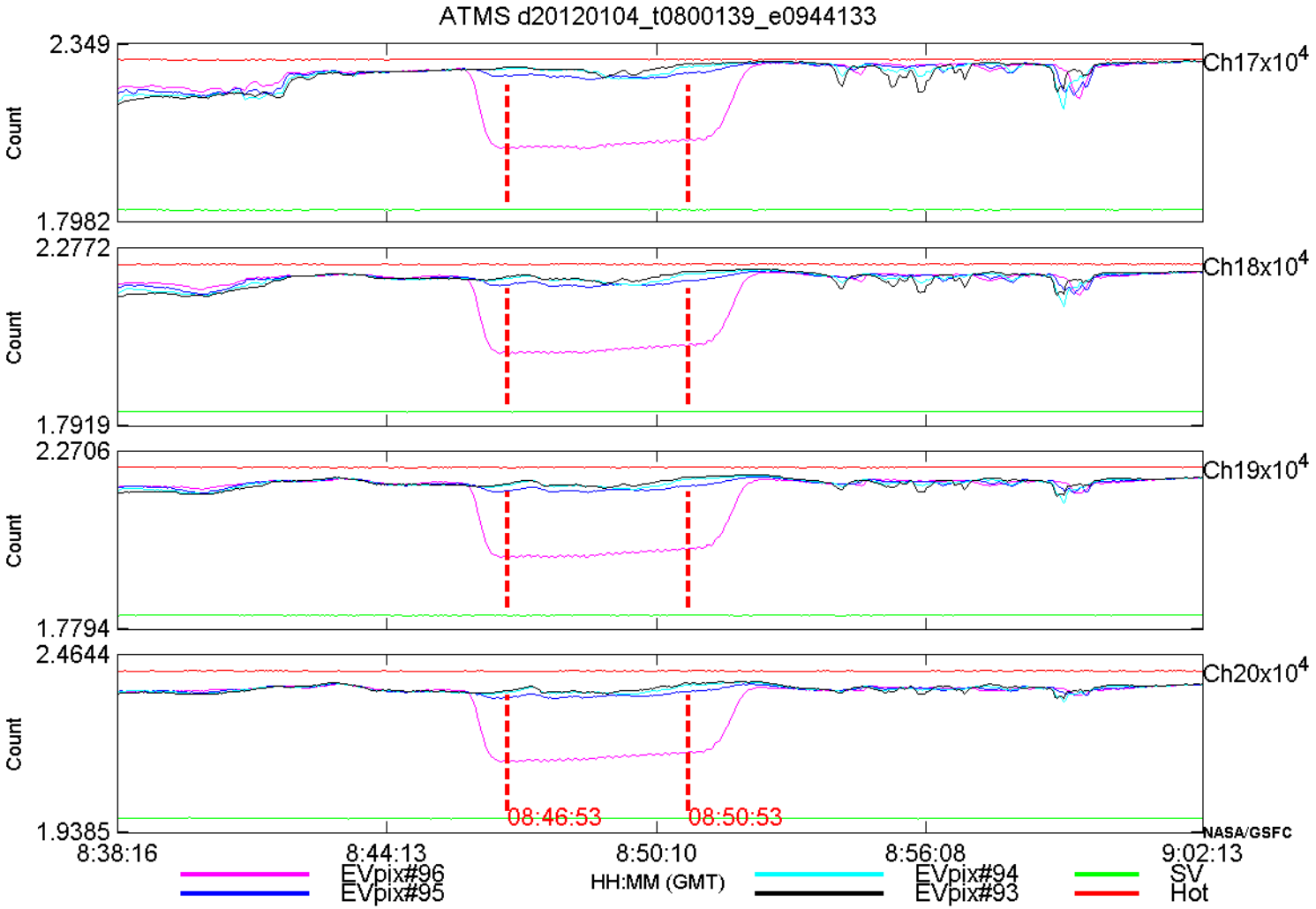

Fig. 7-2. Impacts to ATMS G bands resulting from VIIRS -9.5 deg Lunar Roll.

7.3. Solutions And Recommendations

There are two potential solutions:

Solution #1: We simply flag the VIIRS maneuver events and discard these contaminated and/or uncontaminated scans, because ATMS sensor deviated from its nadir view, then for -9.5 deg roll we would lose, at most, about 12 min worth of TDR, calibrated SDR, Re-map SDR, and EDR data products during this time. In this case, considering other sensors' yaw and pitch maneuver events, we would lose a lot of ATMS SDR/EDR related data products.

Solution #2: We discard only the contaminated EV pixels and process all the uncontaminated EV pixels during VIIRS lunar maneuver and/or other sensors' maneuver events.

We recommend that we adopt **solution #2** in the next IDPS (MX 5.2 built) processing.

8. Nadir Stare for Geolocation Improvement

8.1. (Potential) **Task #27 Objective**

(Note: In the NPP/ATMS OPSCON, there are only 25 assigned tasks)
Determine geolocation to fix the geolocation error in current TDR descending data.
Responsible Teams: NASA(Co-Primary), Other ??? Teams (CP)
Exit Criteria:
A short-term geolocation mitigation plan is prepared and executed.

8.2. Background

Currently there are **two tasks** to work on geolocation issues.
Task 16 – **Geolocation Verification** to evaluate the pitch, roll, and yaw accuracy of the native ATMS FOVs in a traditional method. Tabulate radiometric water/land crossings for more than 3 months. This will indicate whether geolocation is within acceptable limits and to derive an alignment error correction. For **window channels**, we may be able to derive geolocation and navigation accuracy. However, for **non-window channels**, we could depend only on pre-launch tests (OPSCON Sec. 10.18).

An **un-assigned Task VER-4** (ATMS OPSCON Sec. 10.22) – **Geolocation Brightness Temperature Comparison** to determine pointing, navigation, and asymmetry errors. In this task, global SDR brightness temperatures will be binned and averaged in 0.5 deg lat-lon boxes separately for ascending and descending nodes. These values will be differenced. Any systematic pointing or navigation errors will be revealed by shadows on opposite sides of continental coastlines. **Perhaps** we could find the geolocation differences during day/night measurements. This could be used as **a sanity check**.

To correct the **geolocation errors in TDR data** (see **next few pages**), the **nadir stare mode**, on the other hand, is a very important early on-orbit checkout test, since it is by far the quickest and most accurate way of determining **pitch** and **roll** pointing in a short time (i.e. without having to wait to accumulate a large amount of data sufficient to form a high fidelity surface image). **Bjorn Lambrigtsen** (JPL) described this test in his paper on **co-alignment of the AIRS system** (IEEE TGRS, vol 41, 343-351, 2003).

The Nadir Stare method was developed after the Aqua launch to verify the pointing of both AMSU-A and HSB, and the method works very well and is very accurate. It is necessary for ATMS to stay in stare mode for 24 – 48 hours, to ensure that a sufficient number of unobscured coastline crossings with suitable crossing geometry can be obtained.

One caveat for (tradition method) using ATMS assigned FOV centered geolocation to match the coastline is that before comparisons, we have to project exact ATMS footprint sizes of each corresponding pixels on the ground in the global map (see red circle below). For instance, if we match the one footprint (FOV) geolocation center to the geolocation of the coastline (see **blue circle** below), then the brightness measured at this (**blue**) footprint would represent the average brightness temperature of both ocean and land.

We assign derived geolocation to the sensor FOV center

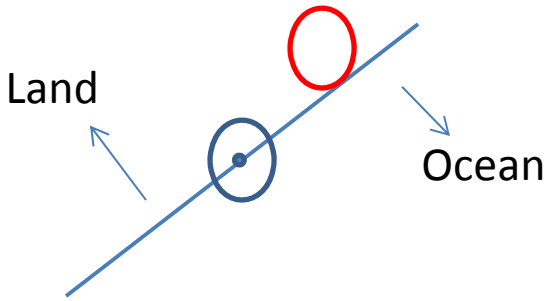

In fact, a spacing is between the sensor FOV center and coastline geolocation.

8.3. Problem In ATMS Descending Geolocation???

In ATMS projection maps, we don't seem to have any geolocation problem for ATMS ascending scanning data. However, we do find some **geolocation shifted map** in ATMS **descending** data (see below a descending **map**).

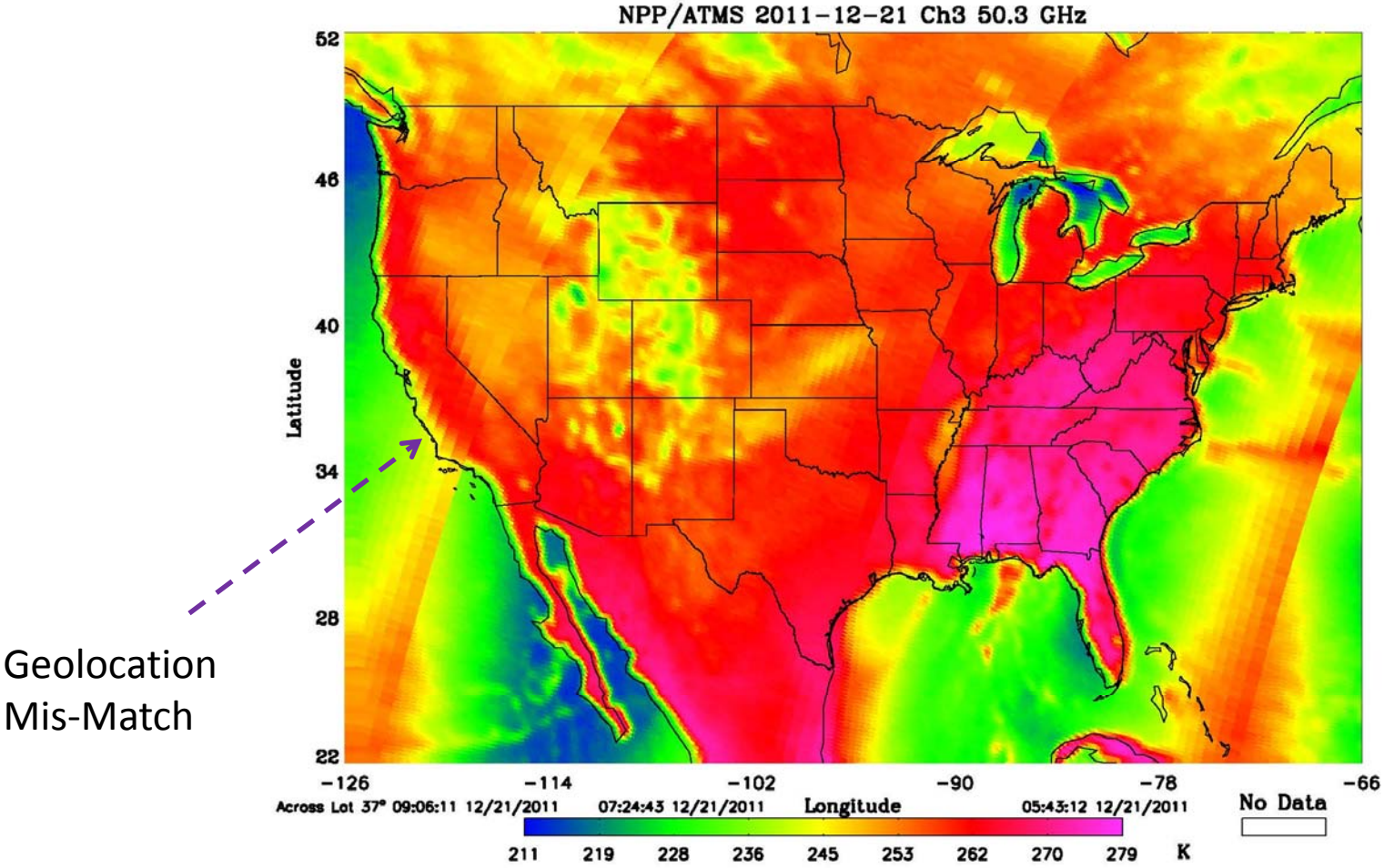

Fig. 8-1. ATMS **Descending** Ch 3 Image of USA/Canada/Mexico on Dec. 21, 2011.

In ATMS **ascending** map, we would find clear distinction between coastlines and ocean areas. The geolocation data in this coarse USA map are quite accurate.

ATMS Image lined up with coastlines

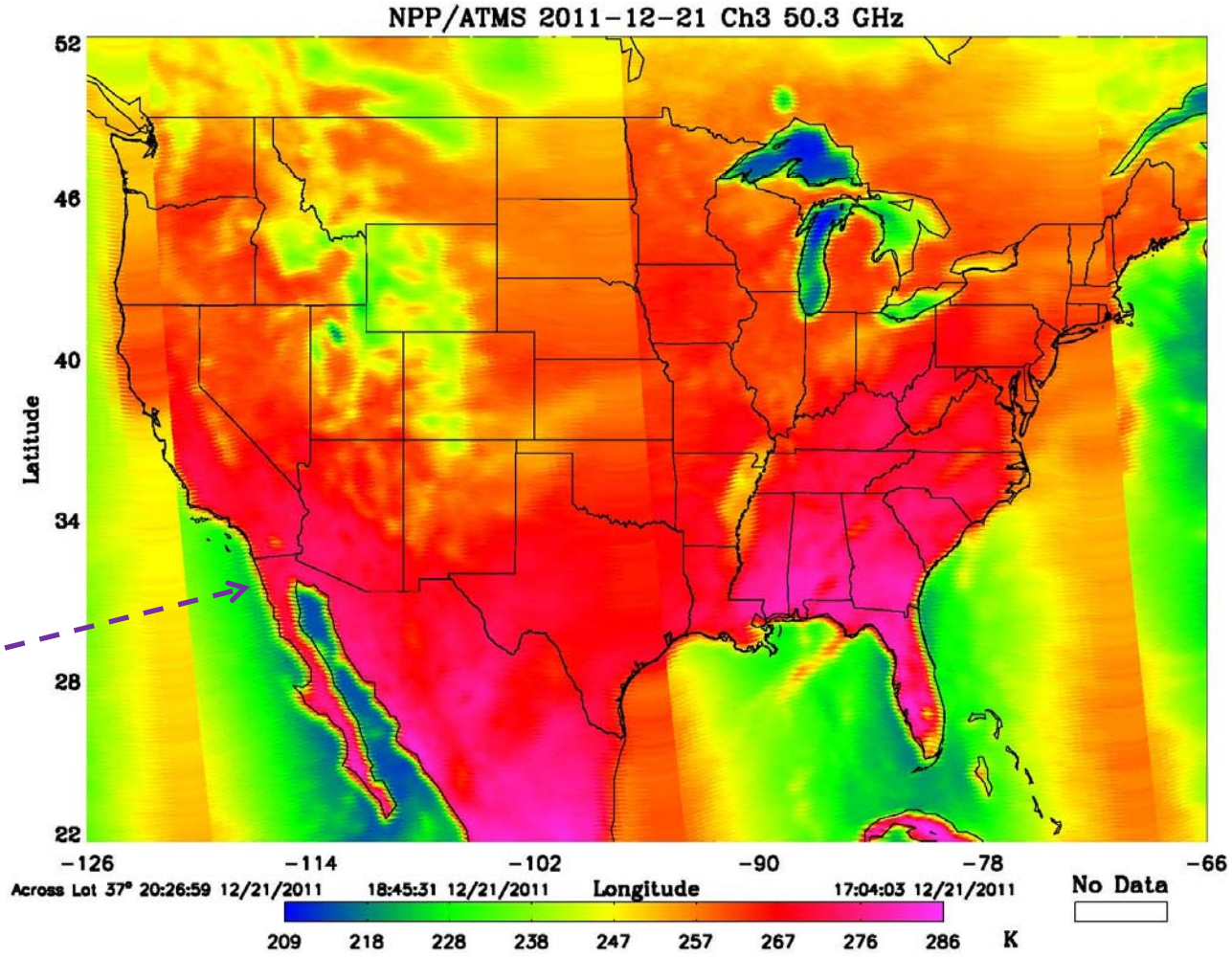

Fig. 8-2. ATMS **Ascending** Ch 3 Image of USA/Canada/Mexico on Dec. 21, 2011.

In ATMS **ascending** map, use H_2O 18 *mm* band Ch 17 to demonstrate again about clear distinction between coastlines & ocean areas. See sharp boundary between Mexico west coast & ocean areas. The geolocation data are so far quite accurate.

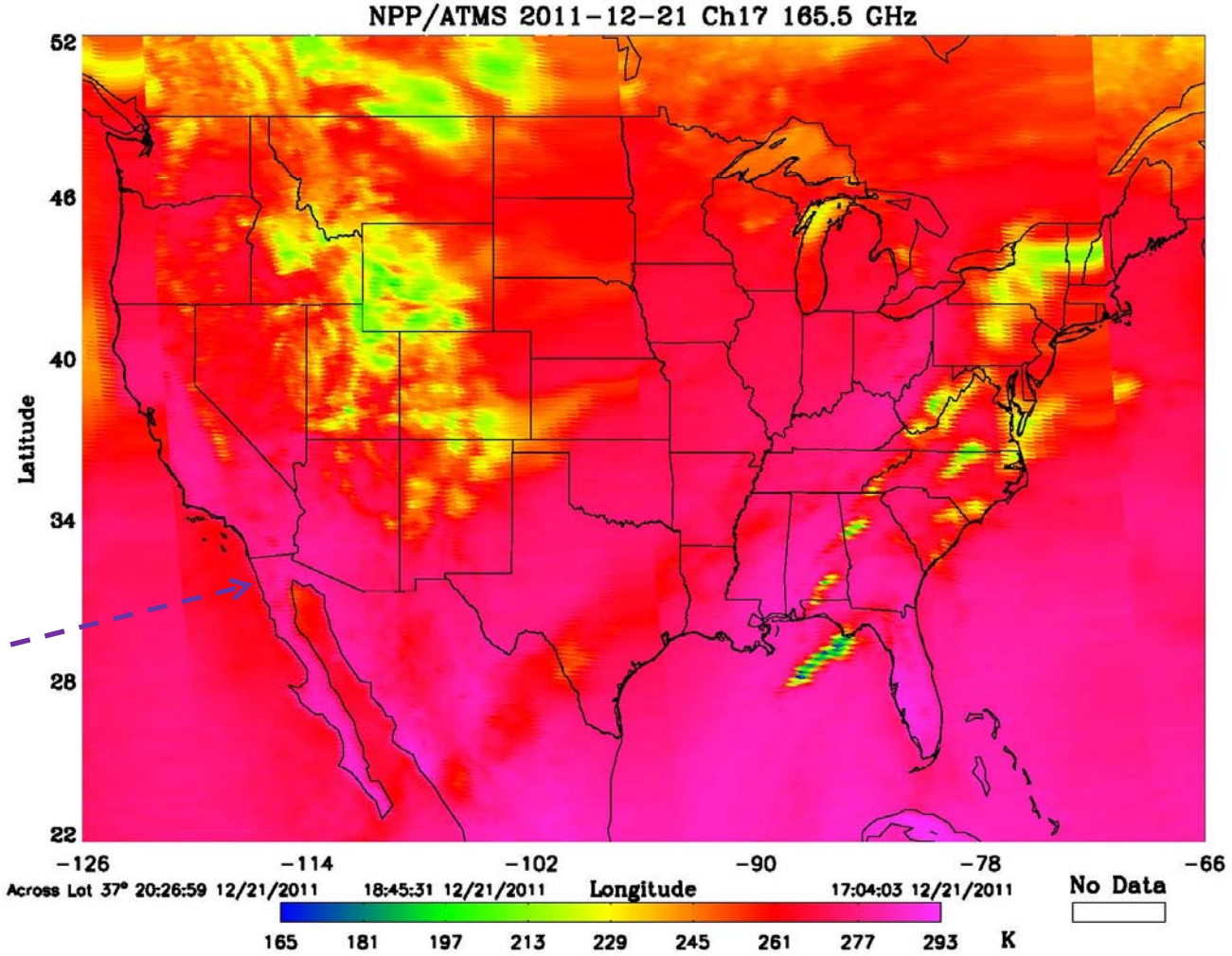

ATMS Image lined up with coastlines

Fig. 8-3. ATMS **Ascending** Ch 17 Image of USA/Canada/Mexico on Dec. 21, 2011.

8.3. Benefits for Nadir Stare

In the 24 hours Nadir stare mode, we can obtain the following benefits:
(1) Determine ATMS geolocation accuracy in two steps.
Use perpendicular coastline cross to calculate the along-track accuracy.
Use the oblique cross case to calculate the cross-track accuracy.

(2) Determine and verify the FOV and antenna beam pointing accuracy.

9. Concluding Remarks/Recommendations

A. In this study, we find that when we switch between different scan profiles, using the difference of SV1 and SV4, i.e., **SV1 – SV4**, would not have any impacts from sensor temperature drifting issues. In this way, we have used an un-biased way to determine that the ATMS optimal scan profile is SP1.

B. From a study of the lunar contamination issues, we recommend that we use all the available SV pixels (at least 1 good SV) to perform sensor calibrations, with the flag indicating that only 1 or 2 good pixels (if applicable, no flag if using more than 3 SV pixels) were used to process SDR and related data products (**Use 2nd proposed method, see p. 33**).

C. Recommend that we **flag/discard only the contaminated EV pixels** during VIIRS monthly lunar and/or other sensors' maneuver events.

D. We recommend we perform **Nadir stare mode** for 24 hours to determine geolocation in a much accurate and faster way. There are additional benefits associated with this nadir stare.

Acknowledgements

On-orbit ATMS data reader and some analysis codes were initially developed by MIT-LL. JPSS DPA/DPE has extensive assistances on post-launch ATMS cal/val tasks. JPSS/NPP MOT and Tina Gentry have assisted us in performing ATMS on-orbit sensor operations and maneuver implementations. Specifically, we would also like to thank Mike Denning, Neal Baker, Wael Ibrahim for assisting us directly on all the ATMS data issues, processing and cal/val tasks.

Backup Slides

SP1

Table 6-1. ATMS lunar intrusion time table predicted by Junqiang Sun from MCST/NICST/NICSE

M/ D/ Y	H: M: S	Rol_ang	SMnSr	E_side
12/3/2011	18:13:31	4.8841	-75.94	N
12/3/2011	19:54:51	4.1168	-75.17	N
12/3/2011	21:36:09	3.3514	-74.4	N
12/3/2011	23:17:25	2.5883	-73.63	N
12/4/2011	0:58:39	1.8276	-72.87	N
12/4/2011	2:39:48	1.0705	-72.1	N
12/4/2011	4:20:53	0.3172	-71.33	N
12/4/2011	6:01:51	-0.4301	-70.56	N
12/4/2011	7:42:38	-1.168	-69.79	N
12/4/2011	9:23:08	-1.8899	-69.01	N
12/4/2011	11:03:11	-2.5871	-68.21	N
12/4/2011	12:42:26	-3.2397	-67.39	N
12/4/2011	14:20:12	-3.8056	-66.5	N
12/4/2011	15:55:34	-4.1946	-65.45	D
12/4/2011	17:28:50	-4.2754	-64.23	D
12/4/2011	19:03:02	-4.0135	-63.11	D
12/4/2011	20:39:51	-3.515	-62.17	D
12/4/2011	22:18:34	-2.8947	-61.33	D
12/4/2011	23:58:19	-2.2155	-60.54	D
12/5/2011	1:38:40	-1.5055	-59.77	D
12/5/2011	3:19:20	-0.7782	-59	D
12/5/2011	5:00:13	-0.0407	-58.24	D
12/5/2011	6:41:15	0.7046	-57.48	D
12/5/2011	8:22:23	1.4544	-56.72	D
12/5/2011	10:03:35	2.2066	-55.96	D
12/5/2011	11:44:50	2.9605	-55.2	D
12/5/2011	13:26:08	3.7161	-54.44	D
12/5/2011	15:07:27	4.4736	-53.68	D

SP1

Table 6-2. ATMS lunar intrusion time table

M/ D/ Y	H: M: S	Rol_ang	SMnSr	E_side
1/2/2012	15:44:56	4.9819	-75.4	N
1/2/2012	17:27:21	4.4784	-74.6	N
1/2/2012	19:09:52	4.0099	-73.78	N
1/2/2012	20:52:29	3.5806	-72.95	D
1/2/2012	22:35:11	3.196	-72.12	D
1/3/2012	0:18:00	2.8636	-71.28	D
1/3/2012	2:00:55	2.5906	-70.42	D
1/3/2012	3:43:55	2.3837	-69.56	D
1/3/2012	5:26:59	2.2491	-68.69	D
1/3/2012	7:10:05	2.1898	-67.82	D
1/3/2012	8:53:12	2.2057	-66.95	D
1/3/2012	10:36:18	2.2958	-66.08	D
1/3/2012	12:19:20	2.4598	-65.21	D
1/3/2012	14:02:18	2.6939	-64.35	D
1/3/2012	15:45:11	2.9925	-63.5	D
1/3/2012	17:27:57	3.3495	-62.66	D
1/3/2012	19:10:38	3.7554	-61.83	D
1/3/2012	20:53:12	4.2047	-61.01	D
1/3/2012	22:35:41	4.6917	-60.19	D

Dec. 6-7 SV1 Diurnal variation was removed Dec. 6-7 SV4

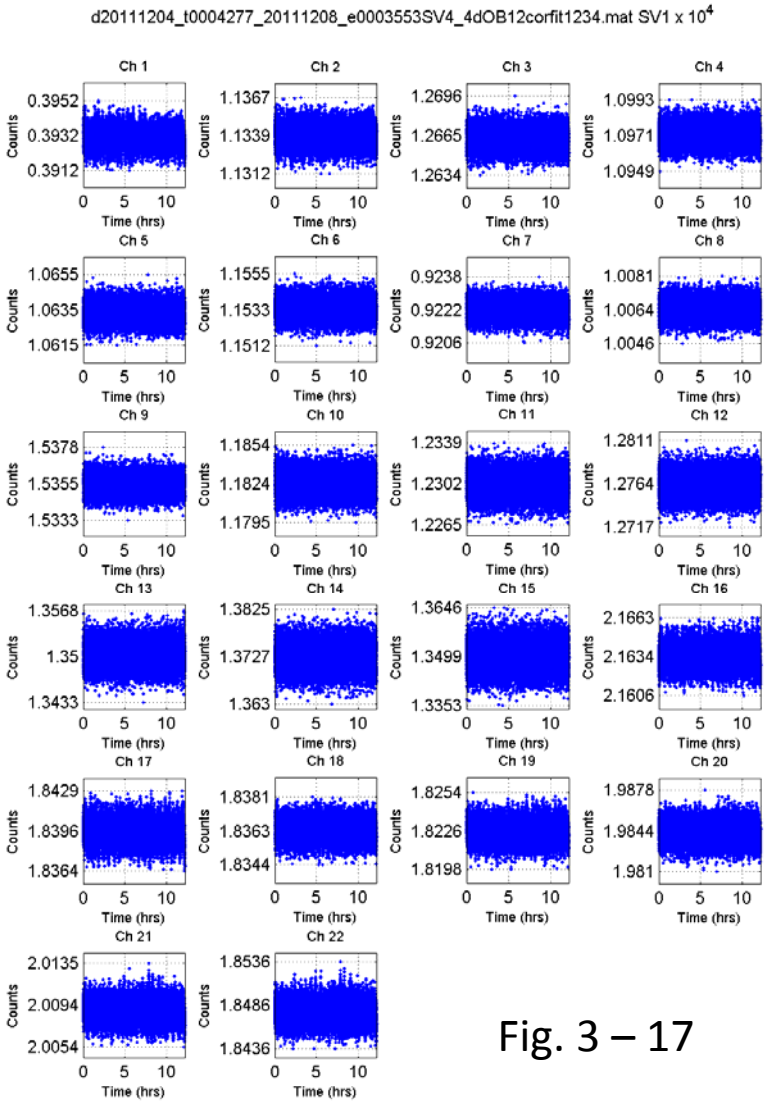

Fig. 3 – 17

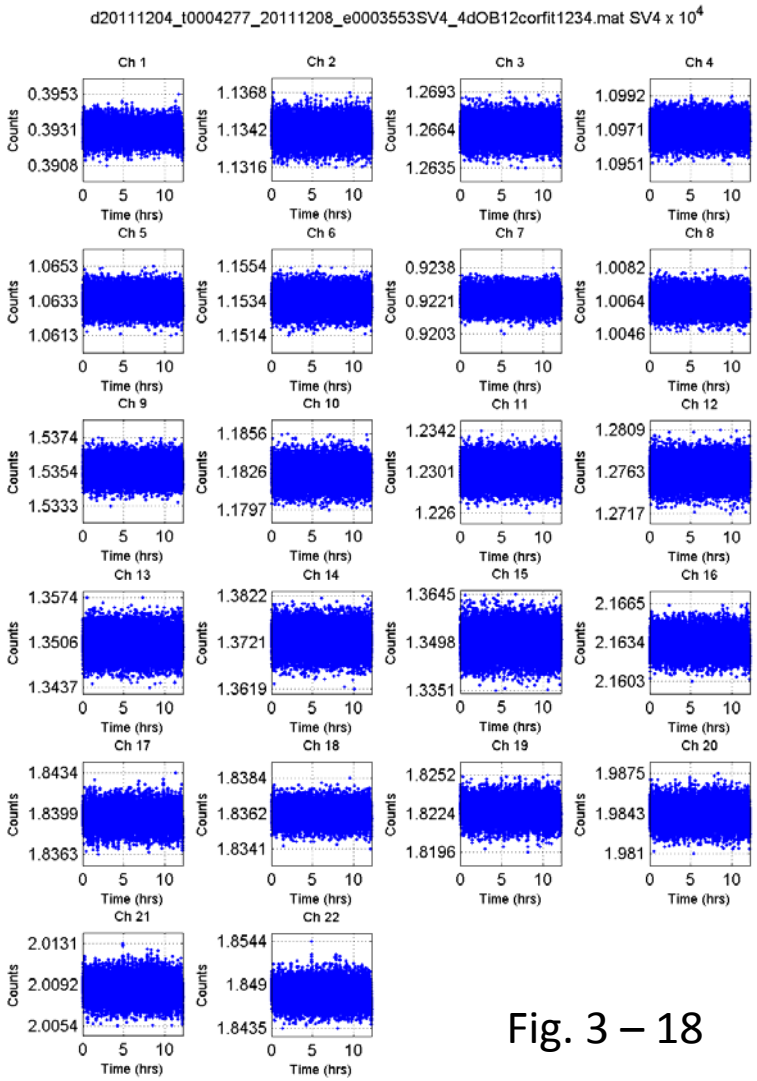

Fig. 3 – 18

The half orbital noise component was also removed. The σ is reduced. See page 10 for comparisons.

SP1

Nov. 18 **SV4** Diurnal variation was removed **SV4** Nov. 19

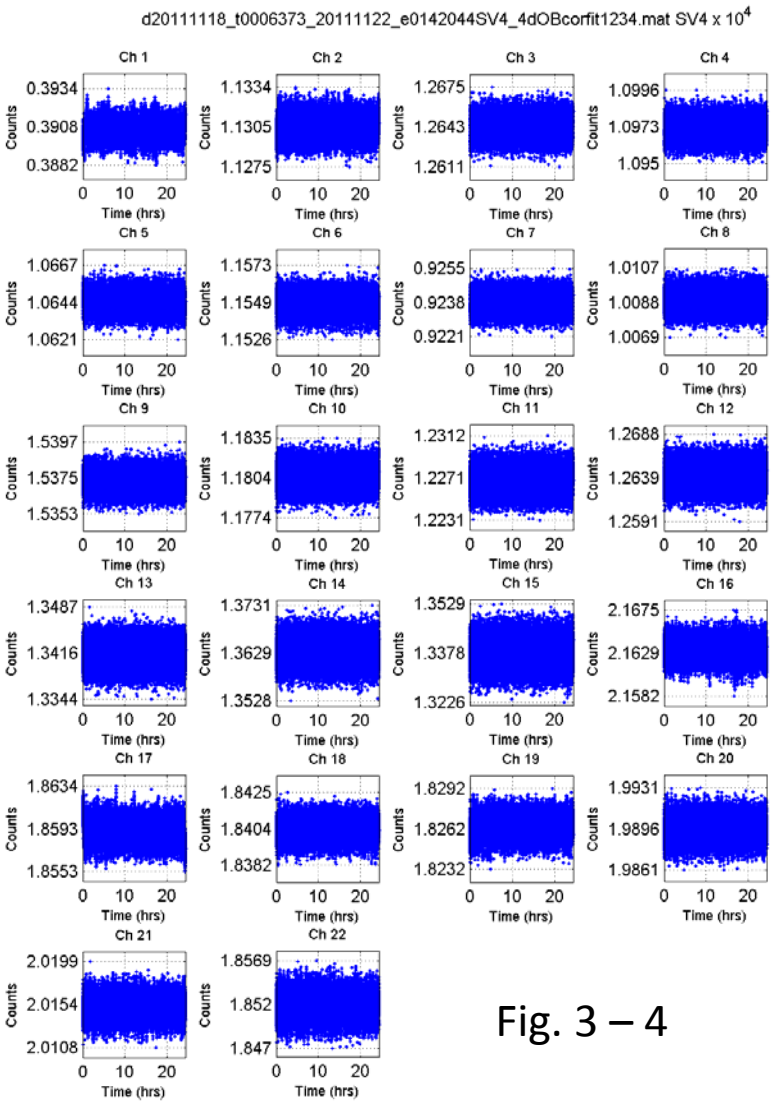

Fig. 3 – 4

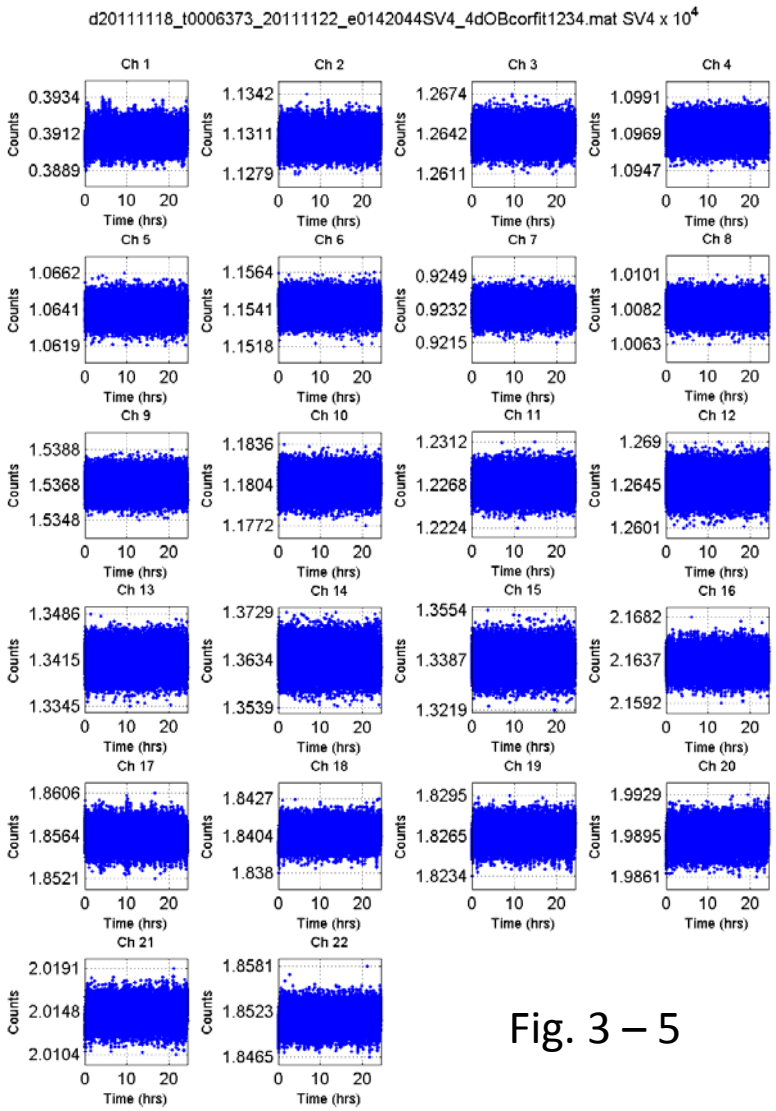

Fig. 3 – 5

Comparing two different 24 hours data sets, here shows SP1 repeatability result.

SP1

Nov. 26-27 SV1

Diurnal variation was removed

SV4 Nov. 26-27

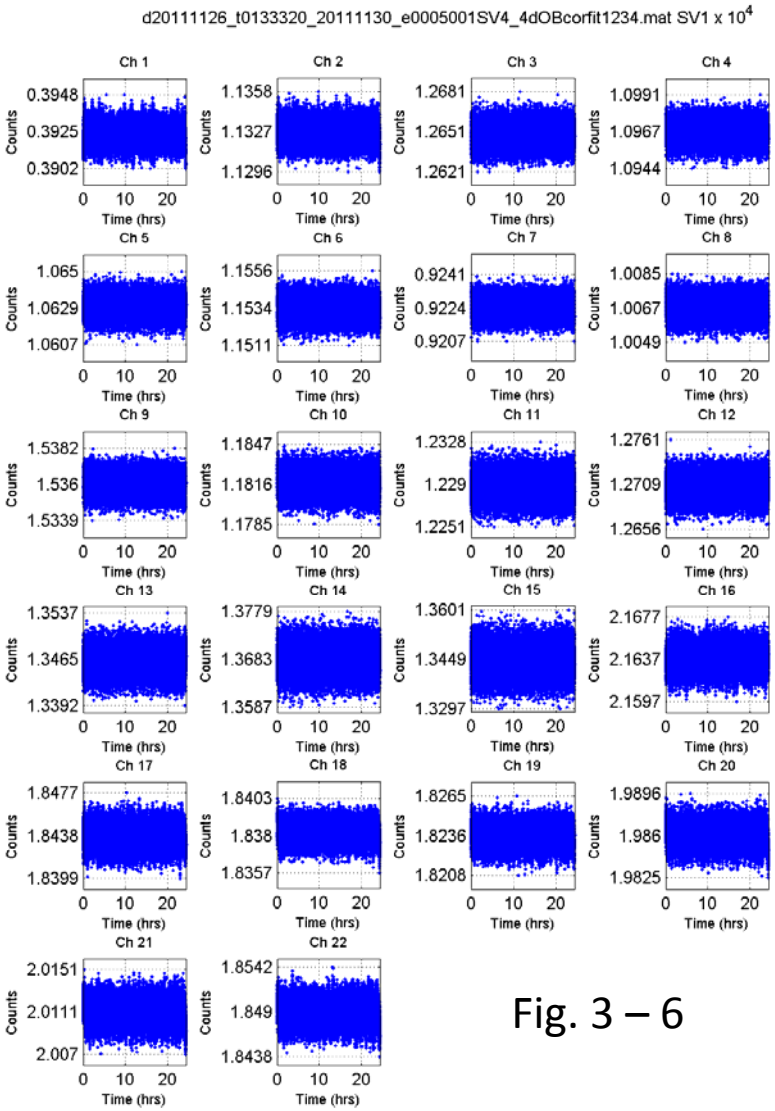

Fig. 3 – 6

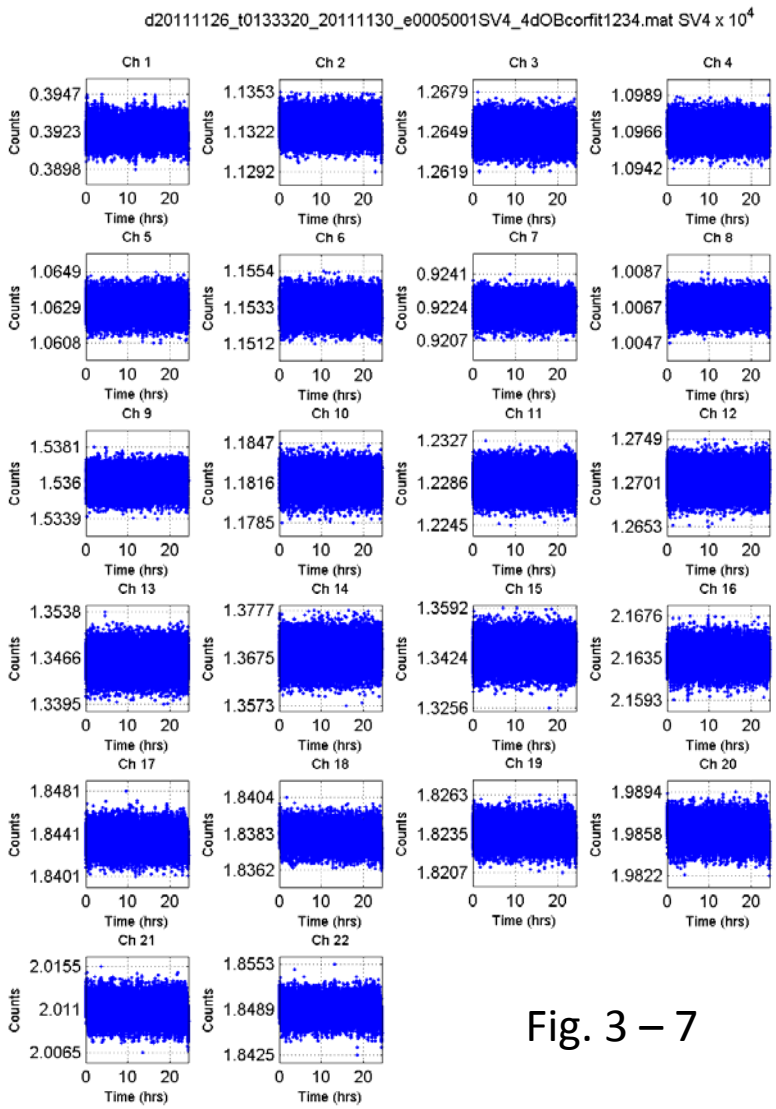

Fig. 3 – 7

SP2

Nov. 29-30 SV1

Diurnal variation was removed

Nov. 29-30 **SV4**

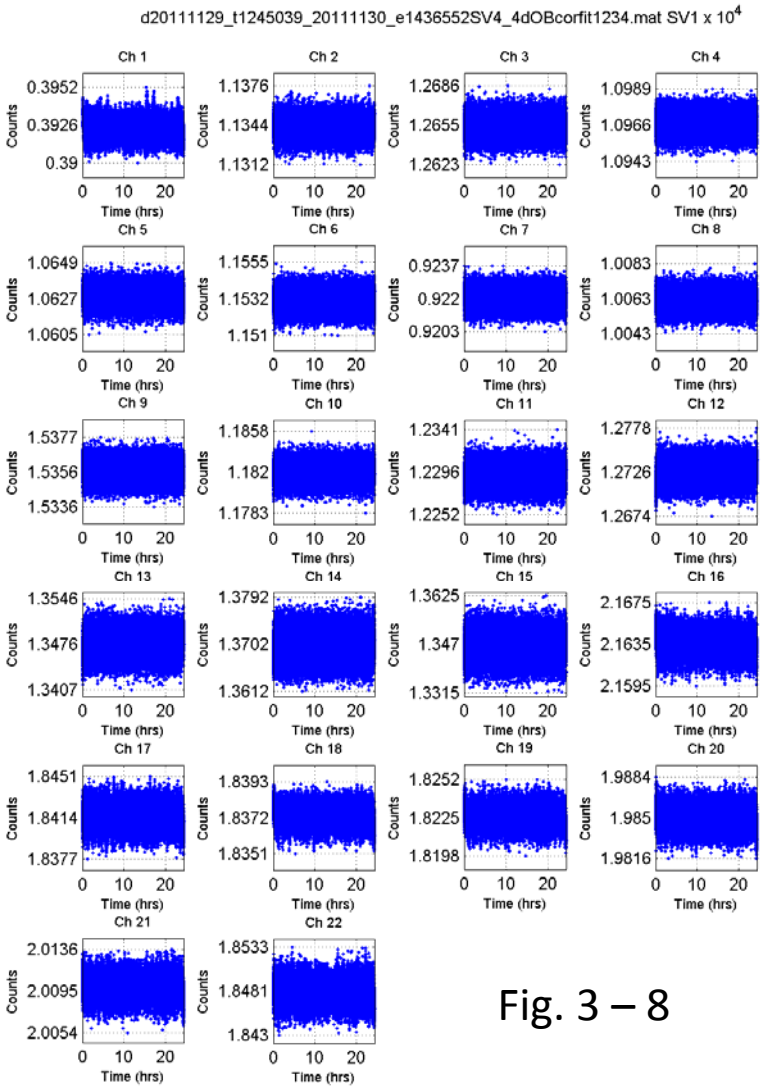

Fig. 3 – 8

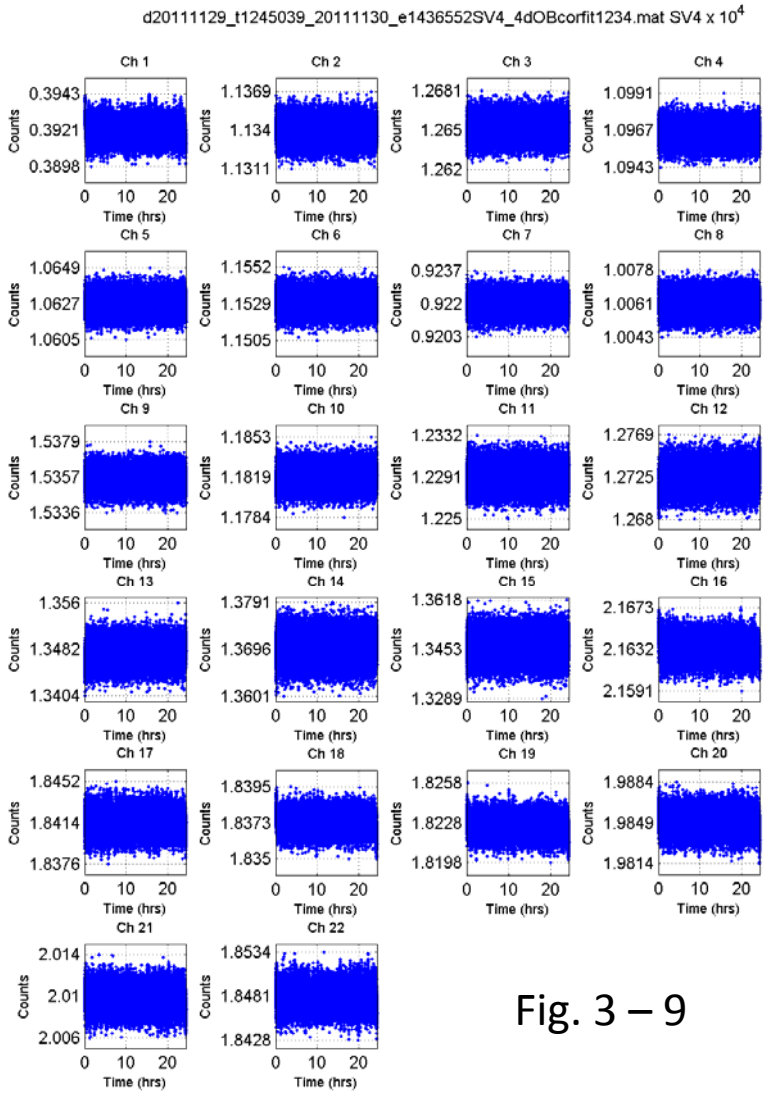

Fig. 3 – 9

SP3

Diurnal variation was removed

Dec. 1-2 SV1

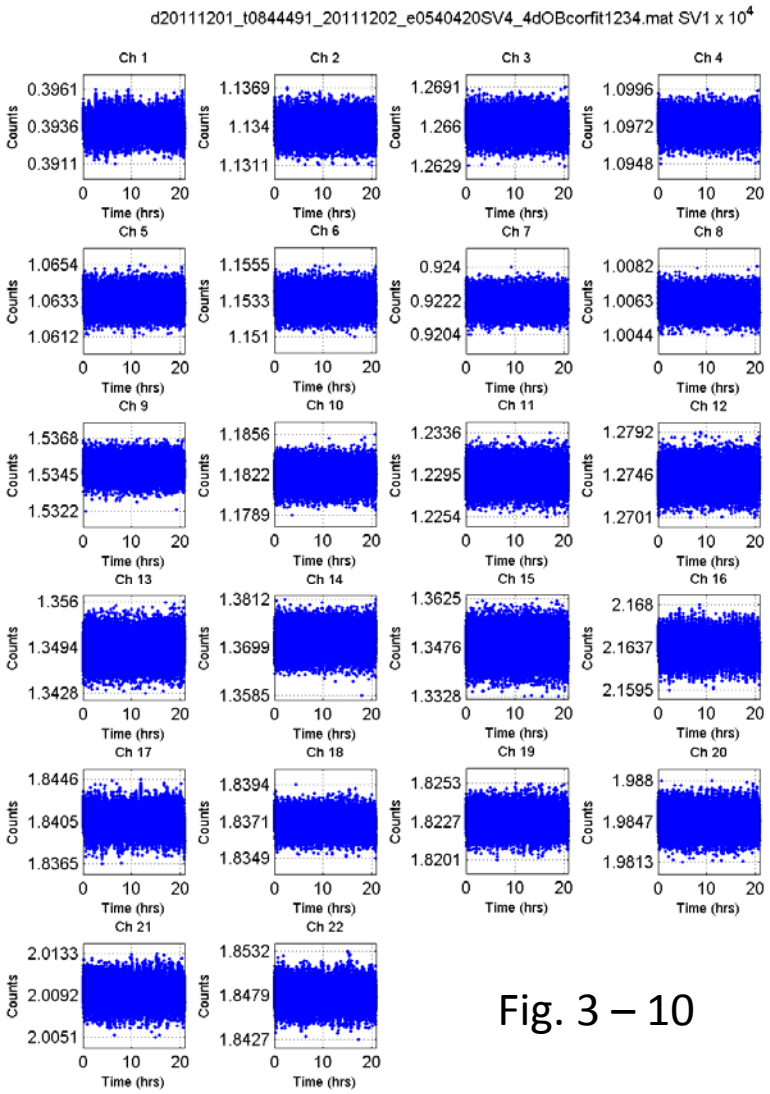

Fig. 3 – 10

Dec. 1-2 **SV4**

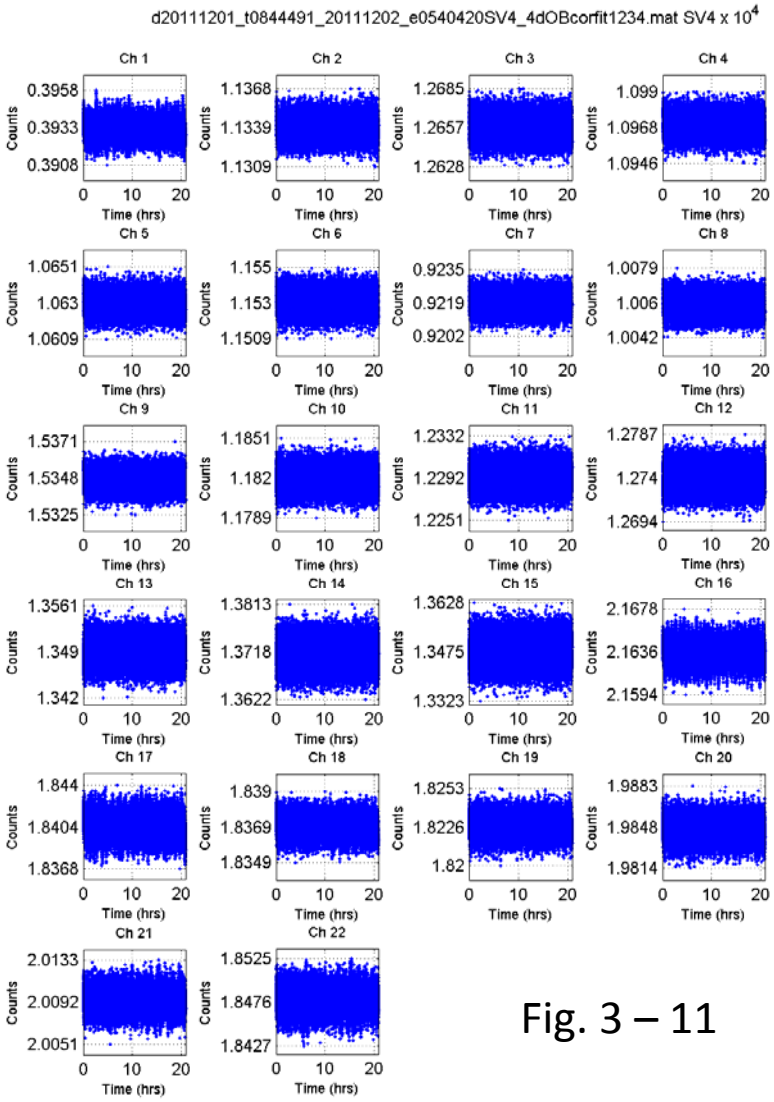

Fig. 3 – 11

SP4

Dec. 8 SV1 **SV4** Table. 3 – 7

Ch	<n>	σ	<n>	σ
1	3929.6,	6.1;	3928.8,	6.0
2	11345.0,	7.2;	11346.4,	7.3
3	12663.8,	7.5;	12664.0,	7.4
4	10975.4,	5.6;	10975.4,	5.6
5	10631.3,	5.1;	10631.5,	5.2
6	11533.1,	5.4;	11533.2,	5.4
7	9220.7,	4.1;	9220.3,	4.1
8	10063.4,	4.7;	10063.2,	4.6
9	15354.1,	5.1;	15353.8,	5.2
10	11830.2,	7.8;	11830.0,	7.8
11	12306.6,	10.1;	12306.1,	10.1
12	12771.9,	11.7;	12771.4,	11.6
13	13511.3,	17.2;	13511.2,	17.0
14	13734.4,	24.4;	13734.9,	24.5
15	13512.0,	38.7;	13510.8,	38.5
16	21628.2,	10.5;	21627.1,	10.1
17	18391.2,	9.2;	18390.5,	9.1
18	18359.2,	5.1;	18358.9,	5.2
19	18223.2,	6.7;	18222.8,	6.8
20	19839.2,	8.5;	19838.8,	8.6
21	20085.6,	10.0;	20085.3,	10.0
22	18478.1,	12.2;	18477.5,	12.1

No diurnal variation

SP1 Dec. 8 SV1 **SV4** Table. 3 – 8

Ch	<n>	σ	<n>	σ
1	3929.6,	5.4;	3928.8,	5.4
2	11345.0,	6.9;	11346.4,	7.0
3	12663.8,	7.3;	12664.0,	7.3
4	10975.4,	5.5;	10975.4,	5.5
5	10631.3,	5.0;	10631.5,	5.0
6	11533.1,	5.3;	11533.2,	5.3
7	9220.7,	4.0;	9220.3,	4.1
8	10063.4,	4.6;	10063.2,	4.6
9	15354.1,	5.1;	15353.8,	5.2
10	11830.2,	7.7;	11830.0,	7.7
11	12306.6,	10.0;	12306.1,	10.1
12	12771.9,	11.7;	12771.4,	11.5
13	13511.3,	17.1;	13511.2,	17.0
14	13734.4,	24.4;	13734.9,	24.5
15	13512.0,	38.6;	13510.8,	38.5
16	21628.2,	8.1;	21627.1,	7.9
17	18391.2,	8.7;	18390.5,	8.7
18	18359.2,	4.9;	18358.9,	5.0
19	18223.2,	6.4;	18222.8,	6.5
20	19839.2,	8.2;	19838.8,	8.3
21	20085.6,	9.6;	20085.3,	9.6
22	18478.1,	11.7;	18477.5,	11.6

No diurnal & half orbital variation